Mineralogy and Petrology (2023) 117:663–683
https://doi.org/10.1007/s00710-023-00817-2

ORIGINAL PAPER

Interpretation of wide zircon U–Pb age distributions in durbachite-type Variscan granitoid in the Mórágy Hills

Annamária Kis[1,2] · Tamás G. Weiszburg[1] · István Dunkl[3] · Friedrich Koller[4] · Tamás Váczi[1,5] · György Buda[1]

Received: 9 August 2021 / Accepted: 14 February 2023 / Published online: 24 March 2023

Abstract

In situ U–Pb analyses were performed on SEM-BSE, SEM-CL and Raman mapped zircons from the Variscan granitoids exposed in the Mórágy pluton, Hungary. However, the routinely used LA-ICP-MS could result only in reliable age constraints if the system was not overprinted by multiple geological processes that affect the isotope system of zircons. To overcome the ambiguities the new zircon U–Pb age data were evaluated carefully, first using simple statistical models, then a zircon internal texture related complex approach was applied. This method demonstrates that the U–Pb age in overprinted systems correlates with the structural state; the worse structural state zones showing younger, but still concordant ages. Individual zircon internal texture and structural state based evaluation made it possible to select the least overprinted age components of the system and identify five steps in the evolution of the studied intrusive rock. The two melts (granitoid and mafic) passed the zircon U–Pb isotope closure temperature ~ 355 ± 3 Ma ago during their cooling. Crystallization of the two mingled magmas overarched the 350–340 Ma period, including two intense zircon crystallization peaks (~ 347 Ma, ~ 333 Ma). The cessation of melt crystallization (~ 650 °C) happened ~ 334 ± 4 Ma ago, as indicated by the age of the "normal and long prismatic" zircons. Further confirming this statement, they are embedding in their rims the eutectic mineral assemblage. A Cretaceous post-magmatic event was identified according to slightly discordant U–Pb ages for the Mórágy pluton.

Keywords Zircon structural state · U–Pb concordance · Metamorphic overprinting · Mórágy granitoid · Tisza Mega-unit

Introduction

Zircon has been widely used to decode both the geochemical and geochronological backgrounds of samples (Hoskin and Schaltegger 2003; Cherniak and Watson 2001, 2003; von Quadt et al. 2014). Along with this benefit, it is true that some zircon grains can have inhomogeneous textures or heterogeneous distribution of U–Pb isotopes (e.g. Friedl et al. 2004; Hattori et al. 2017). Chang et al. (2006), Schmitt et al. (2010) and von Quadt et al. (2014) equally reported that the U–Pb age determined from an thin overgrowth layer of a zircon crystal was significantly younger than that determined from the core of the zircon. This can be explained either by the secondary growth of the rim through a magmatic process or by the delay of the start of U–Pb chronometer attributable to isotopic diffusion caused by decompression or by rapid cooling in the host magma. Several pioneering studies have revealed that in-situ U–Pb isotopic analysis can provide reliable chronological information (Schmitt et al. 2010; Lowenstern et al. 2000; Gallhofer et al. 2016; Hattori et al. 2017). In our present work, we used U–Pb dating of zircon crystals to solve a similar problem that is unique in terms of the geographic setting of the granitoid.

Extensive discussion concerning the origin of mafic enclaves in Variscan "durbachite-type" granitoid of Hungary's Mórágy Hills pluton has long been based mainly on petrological and

Editorial handling: A. Möller.

✉ Annamária Kis
annamari.kis@gmail.com

[1] Department of Mineralogy, Eötvös Loránd University, Budapest, Hungary

[2] Department of Mineralogy and Petrology, Hungarian Natural History Museum, Budapest, Hungary

[3] Department of Sedimentology and Environmental Geology, Geoscience Center, University of Göttingen, Göttingen, Germany

[4] Department of Lithospheric Research, University of Vienna, Vienna, Austria

[5] Department of Applied and Nonlinear Optics, Institute for Solid State Physics and Optics, Wigner RCP of the H.A.S., Budapest, Hungary

geochemical constraints (Buda 2001; Buda and Dobosi 2004; Király and Koroknai 2004). Comparative age determinations were valuable contributions to clarifying that issue, these age data, however, fell short of answering basic questions. The main reason for this being the ambiguity due to unclear heterogeneity of the studied zircon crystals. As of yet, in-situ texture related zircon U–Pb age data are not available for the rock types of this magmatic complex.

A major setback to obtaining properly time-resolved and reliable zircon age data is in fact the internal inhomogeneity of the zircon crystals themselves. The complex, texture-related local chemical and structural pre-examination of zircon crystals must by all means be taken into account before dating (Kis et al. 2019).

In this paper we focus on the identification and clarification of various geological events based on their traces preserved in zircon textures from different granitoids. We analyzed one hundred eighty carefully pre-selected (Kis et al. 2019), non-metamict spots in ninty eight zircon crystals using laser ablation inductively coupled plasma mass spectrometry (LA-ICP-MS).

Our major goal is the zircon internal texture related U–Pb zircon age determination of the three primary magmatic rock types from Mórágy Hills, time-resolved enough for allowing the interpretation of the genetic relationship of the three. We also investigate potential inherited ages (Klötzli et al. 2004) in the antecrystic/xenocrystic cores of our zircons. Finally, by processing part of the discordant age data sets we attempt to find and interpret the traces of secondary, overprinting geological process in the locality (Király and Koroknai 2004; Haas et al. 2014). As a conclusion, we achieve a more refined genetic interpretation of the magmatic processes as a contribution to the pasting between the "durbachite"-type Variscan plutonic rocks in Europe.

"Durbachites" - geological setting of Mórágy intrusion

The magnesio-potassic granitoids with high-potassic mafic enclaves are widespread in the Variscan collision belt in Europe (Fig. 1), like the so-called "durbachite" in Schwarzwald (Altherr et al. 1999), in Vosges, and in Central and South Bohemian Batholith (Sauer 1892; Holub 1977; Janoušek et al. 1995, 2010; Holub 1997; Gerdes et al. 2003; Parat et al. 2009; Kusiak et al. 2010; von Raumer et al. 2012; Zák et al. 2014; Kubínová et al. 2017; Jastrzębski et al. 2018; Dostal et al. 2019), "vaugnerite" in French Massif Central and in Corsica (Sabatier 1991; Cocherie et al. 1994; Ferre and Leake 2001; von Raumer et al. 2014) or "redwitzite" in the German Fichtelgebirge (Weinschenk 1916).

The studied pluton is exposed in the Mórágy Hills, southern Hungary, in the Tisza Mega-unit (Haas and Péró 2004). The plutonic rocks form an approximately 170 km long and 20 to 30 km wide SW-NE trending, mainly subsurface belt accross the Pannonian Basin, outcropping only nearby the village Mórágy (Kovács et al. 2000; Maros et al. 2004). The Tisza Mega-unit is a dominant structural unit of geodynamic reconstruction and interpretation of the western Neotethyan region (Schmid et al. 2008; Szederkényi et al. 2012). That Mega-unit formed part of the southern margin of the European Plate in the Paleozoic, but its precise paleogeographic position before

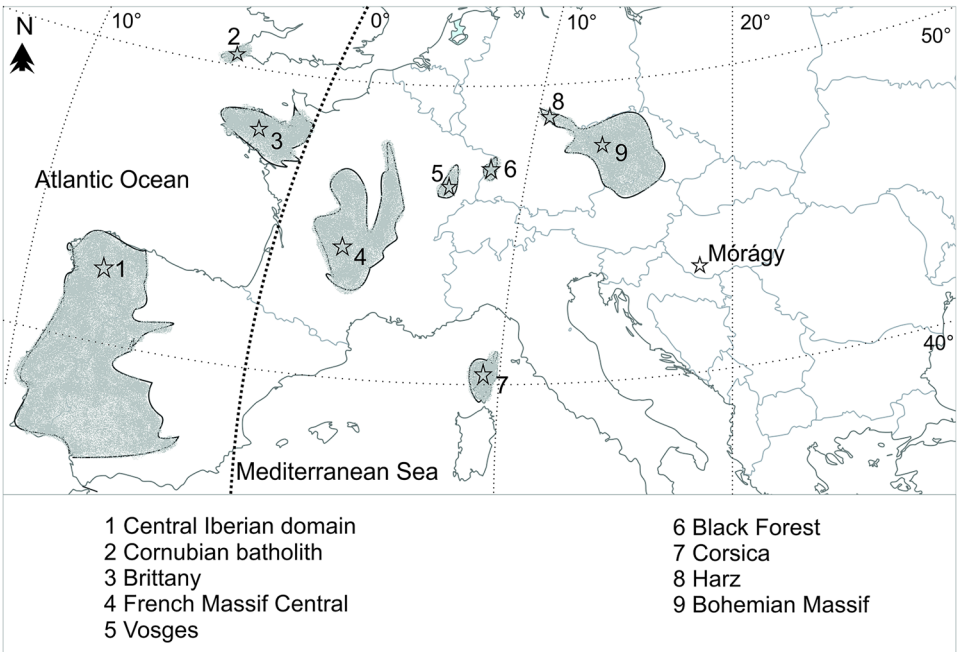

Fig. 1 Current geographical position of the Mórágy (Hungary) pluton and the major "durbachite" occurrences in the European Variscides. Gray patches indicate the Variscan basement areas exposed. Numbered stars refer to the pluton names in legend (after Faure et al. 2014)

the Jurassic continental rifting is still widely disputed. Szulc (2000), Götz and Török (2008) suggest it was situated to the east of the Bohemian Massif. Csontos and Vörös (2004), Haas and Péró (2004) position the Mega-unit to the western part of the Neotethyan shelf, south of the Bohemian Massif. According to Tari (2015) the Tisza Mega-unit was situated west of the Bohemian Massif. Later, in the Early Bathonian, Jurassic (Géczy 1973; Haas and Péró 2004) the Mega-unit was separated from the European Plate by the Tethyan rifting.

That pre-Alpine basement built up – beside the plutonic rocks – polymetamorphic gneisses, micaschists, amphibolites. Radiometric age and petrology testifies to three distinct metamorphic events in these rocks: pre-Variscan (440–400 Ma, high P, medium T), Variscan (350–330 Ma, medium PT) and late- to post-Variscan (330–270 Ma, low P, high T) (Büttner and Kruhl 1997; Henk et al. 2000; Klötzli et al. 2004).

The granitoids of the Mórágy pluton are characterized mainly by metaluminous, I-type and slightly peraluminous, S-type, calc-alkaline, high-K and high-Mg ultrapotassic intrusions and enclaves (Bea et al. 1999; Buda and Nagy 1995; Buda et al. 2000; Buda and Dobosi 2004; Klötzli et al. 2004; Buda and Pál-Molnár 2012, 2014). Geochemical and petrological characteristics of the pluton shows strong resemblance with durbachitic K-Mg-rich plutonic series of the Bohemian Massif, like the Čertovo břemeno intrusive and the Třebíč pluton (Janoušek et al. 1995, 2010; Holub 1997; Kusiak et al. 2010; Zák et al. 2014).

Rock types and hosted zircons

The petrography of Mórágy pluton is well documented (Szederkényi 1977; Jantsky 1979; Buda et al. 1999, 2012, 2014; Király and Koroknai 2004, Klötzli et al. 2004). The pluton is experienced Permian amphibolite facies post-emplacement metamorphism (Szederkényi 1996; Király and Koroknai 2004; Lelkes-Felvári and Frank 2006) which brought about biotitisation and microcline-replacement texture and in the early Cretaceous extension-related alkaline magmatism happened next to the pluton (Kovács et al. 2000; Haas et al. 2014).

We have studied the three dominant rock types: (1) host, microcline megacryst-bearing granitoid, (2) mafic enc1ave, that was influenced by potassium enrichment (Buda 2001; Buda and Dobosi 2004), and (3) hybrid rock, forming a narrow transition zone between the host rock and the enclaves (Fig. 2). Earlier petrographical, geochemical and geochronological data prove that the three different rock types of the Mórágy intrusion are cogenetic (Király and Koroknai 2004; Koroknai et al. 2010).

Three prismatic morphology types of zircons (Pupin 1980; Kebede et al. 2001) were identified by Klötzli et al. (2004): normal prismatic (S_{24}, S_{25}), short (AB_5) ("flat" by Klötzli et al. 2004: re-defined by Kis et al. (2019) from S_4 to AB_5) and long prismatic (P_5).

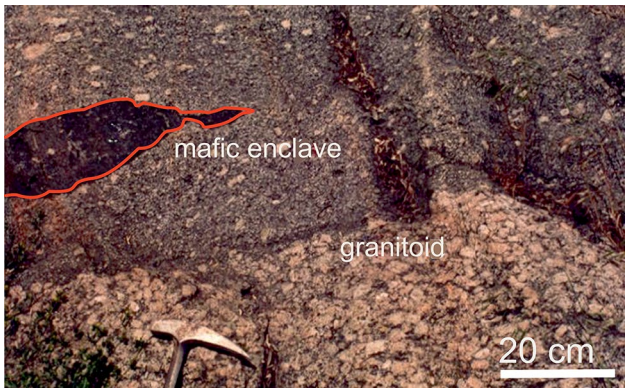

Fig. 2 Outcrop-scale field observation of the typical lithologies from Mórágy Hills, Bátaapáti quarry. Red lines indicate the contour of mafic enclaves (after Kis et al. 2019)

Earlier geochronological studies on Mórágy pluton

A wide range of geochronological data are available for the primary magmatic rocks of the Mórágy pluton (Ovchinnikov et al. 1965; Kovách et al. 1968; Árva-Sós and Balogh 1979; Svingor and Kovách 1981; Balogh et al. 1983; Chernüsov 2002; Klötzli et al. 2004; Shatagin et al. 2005; Koroknai et al. 2010; Fig. 3). Klötzli et al. (2004) determined 354 ± 5 Ma on the normal prismatic zircons by evaporation Pb-Pb method, while their short prismatic zircon indicated younger U–Pb age (339 ± 10 Ma), based on ion microprobe U–Pb analysis. Shatagin et al. (2005) determined the age of crystallization (405 ± 4 Ma) by TIMS U–Pb dating on one perfectly concordant zircon fraction of the host granitoid rock. Koroknai et al. (2010) reported zircon age data using laser ablation magnetic sector field inductively coupled plasma mass spectrometry (LA-SF-ICP-MS) technique and confirmed the Variscan age of the Mórágy pluton. Their samples were taken from both the host granitoid rock and the mafic enclave. They did not find inherited cores, and their "normal" prismatic, oscillatory zoning zircons showed U–Pb age 339 ± 3 Ma and Pb-Pb age 343 ± 9 Ma.

Samples and analytical methods

Sample preparation and optical petrography

Approximately 5 kg of unweathered rock samples were collected from boreholes (Üh-1, 48 m, 54 m, 118–119 m,

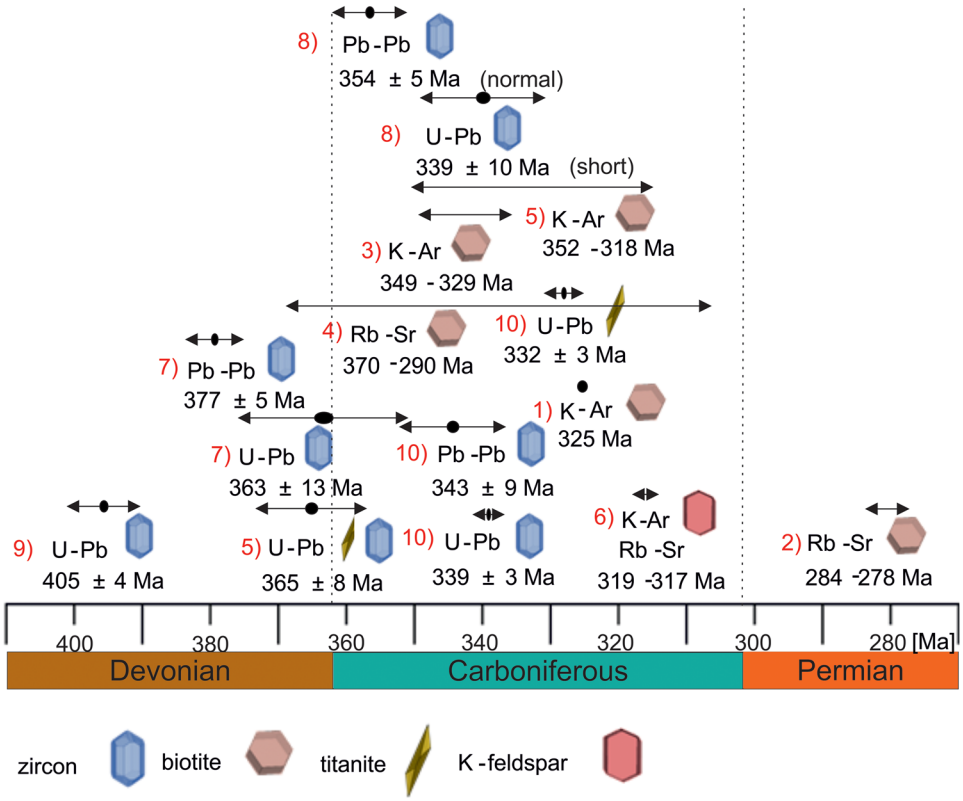

Fig. 3 Compilation of published geochronological data obtained by different mineral-method pairs from the Mórágy pluton. 1) Ovchinnikov et al. 1965, 2) Kovách et al. 1968, 3) Árva-Sós and Balogh 1979, 4) Svingor and Kovách 1981, 5) Balogh et al. 1983, 6) Chernüsov 2002, 7) Klötzli et al. 2004, 8) Shatagin et al. 2005, 9) Koroknai et al. 2010

158 m). The zircon crystals were concentrated by the standard techniques combining crushing, sieving, magnetic and heavy liquid separation and hand picking in alcohol under stereomicroscope. The color, opacity and crystal habit were recorded for each selected grain. Zircons of all three rock types were grouped according to their external morphology (Pupin 1980). We found in all three rock types, all three morphological zircon types (normal (S_{24}, S_{25}), short (AB_5), long (P_5) prismatic) reported by Klötzli et al. (2004).

During a careful pre-selection (Kis et al. 2019) three hundred zircon grains, hundred for each rock type, were embedded in 25 mm diameter epoxy mounts, ground and diamond polished to expose the interior of the grains. All grains were analyzed for internal texture cf. Hanchar and Miller (1993). Then, based on texture grouping hundred nine typical grains, representing the three zircon morphology types of all rock types were selected for structural state determination by Raman spectroscopy (Nasdala et al. 1995, 1998). Within the selected grains three hundred fifty spots were defined for laser ablation analysis, all of them having a structural state < 18 cm^{-1}, characterized by the value of the full width at half maximum (FWHM) of the zircon ν_3 (SiO_4) Raman band (Nasdala et al. 1995, 1998). The spots represented all the internal texture types in the three Mórágy rock types.

After pre-selection of three hundred zircon grains measurements for age dating were performed on 296 spots. According to our measurements, 180 provided concordant ages (Table 1, raw data is in Table S1), 26 slightly discordant ages (Table 2) and additional 90 highly discordant ages (Table S2). The latter ones are not discussed in the manuscript, while concordant and slightly discordant ages are explained in detail.

Apart from the zircon crystal mounts, forty thin sections representing the three rock types of Mórágy pluton (outcrops in Mórágy and Erdősmecske, as well as borehole Üh-1 at 48 m, 54 m, 118–119 m, and 158 m depth) were examined by petrographic microscope, to assess the textural relationship between zircon and the embedding rock-forming minerals.

Scanning electron microscopy (SEM)

Backscattered electron (BSE) and secondary electron (SE) images of zircons were acquired in an AMRAY 1830i SEM instrument at the Department of Petrology and Geochemistry, Faculty of Science, Eötvös Loránd University. The instrument was operated of an accelerating voltage 15 kV, beam current 1 nA.

The internal texture of zircon crystals was meticulously investigated using scanning electron microscope (SEM) techniques (SEM-BSE, SEM-CL, SEM-SE). Cathodoluminescence (CL) images of all polished zircon crystals were acquired in a FEI Inspect S50 SEM instrument located at the Scanning Electron Microscopy and Focused Ion Beam Laboratory, Department of Lithospheric Research, University

Table 1 Concordant ages: number of analysed spots by rock types

Morphology	Internal texture type	Mórágy Hills		
		host (granitoid) rock	*hybrid rock*	*mafic enclaves*
normal prismatic zircon	growth zoning	45	14	15
	core/antecrystic core/xenocrystic core	22	5	5
short prismatic zircon	growth zoning	9	4	5
	core/antecrystic core/xenocrystic core	9	4	5
normal prismatic zircon	sector zoning	3	2	-
normal prismatic zircon	convolute zoning	3	1	2
long prismatic zircon	-	18	3	6
Total		**109**	**33**	**38**

of Vienna, or in a Tescan VEGA SEM instrument at the Geological Survey of Austria (GBA), also in Vienna. Both SEM instruments were operated in low vacuum mode with chamber pressure 25 Pa to minimize charging, an accelerating voltage 10 kV, and a beam current of 1 nA.

Raman spectroscopy

To determine the structural state of zircon zones (value of the full width at half maximum = FWHM) Raman spectroscopy was carried out using the Horiba LabRAM HR UV–VIS-NIR system (Research and Instrument Core Facility, Faculty of Science, Eötvös Loránd University, Budapest). The confocal Raman microspectrometer was equipped with a charge-coupled device (CCD) detector (pixel size 26 µm). Excitation was induced by the 633 nm (17 mW) emission of a He–Ne laser. 100 × microscope objective (Olympus BXFM; numerical aperture 0.9) was used to deliver laser light onto the samples and to collect scattered light. The zero-order diffraction position of the spectrograph and the Rayleigh line (0 cm^{-1} Raman shift) were used for the calibration of the spectrograph dispersion. Raman spectra were evaluated by LabSpec5 software.

Laser-ablation inductively-coupled plasma – mass spectrometry (LA-ICP-MS)

U–Pb geochronological data on the pre-examined zircon crystals were obtained by LA-SC-ICP-MS at the GÖochron Laboratories of Geozentrum, University of Göttingen as described by Frei and Gerdes (2009). The analytical conditions were: spot size 23 µm, crater depth approximately 9–10 µm, repetition rate 5 Hz, energy density ~ 2 J/cm^2 and ablation duration of 20 s (after two cleaning pulses and 12 s of gas blank acquisition). The age calculation was based on the primary standard reference material GJ-1 zircon (Jackson et al. 2004). For further control FC-1 and Plešovice zircons were analyzed as secondary standards (Paces and Miller 1993; Sláma et al. 2008). Drift and fractionation corrections and the data reduction were performed by UranOS software (Dunkl et al. 2008). Two analyte settings were used in data collection. In geochronology optimized setting ^{202}Hg, mass 204, ^{206}Pb, ^{207}Pb, ^{208}Pb, ^{232}Th, ^{235}U and ^{238}U, while in geochemistry optimized setting ^{202}Hg, mass 204, ^{206}Pb, ^{207}Pb, ^{208}Pb, ^{232}Th, ^{235}U, ^{238}U, ^{27}Al, ^{29}Si, ^{31}P, ^{43}Ca, ^{45}Sc, ^{47}Ti, ^{49}Ti, ^{57}Fe, ^{89}Y, ^{138}Ba, ^{140}Ce, ^{173}Yb and ^{177}Hf were

Table 2 Slightly discordant ages: number of analysed spots by rock types

Morphology	Internal texture type	Mórágy Hills		
		host (granitoid) rock	*hybrid rock*	*mafic enclaves*
normal prismatic zircon	growth zoning	4	-	5
	core/antecrystic core/xenocrystic core	1	-	1
short prismatic zircon	growth zoning	1	-	-
	core/antecrystic core/xenocrystic core	2	1	3
normal prismatic zircon	sector zoning	1	-	-
normal prismatic zircon	convolute zoning	1	-	2
long prismatic zircon	-	1	2	1
Total		**26**		

measured. Uncertainties associated with the individual spot ages at the "geochronology optimized" analytical sequences are typically 2–3 Ma for U^{238}/Pb^{206}, while in the "geochemistry optimized" sequences 7–10 Ma, due to the shorter dwell time used for the actinides and Pb isotopes.

Conventional concordia plots (Wetherill 1956) were constructed by Isoplot (Ludwig 2012). Age distributions were tested using the ISOPLOT UNMIX method (Ludwig 2012), based on the algorithm of Sambridge and Compston (1994), using Gaussian distribution for the age components. Statistical confirmation of the number of age populations was performed by t-test (Pearson 1939).

Results

Suitable zircon crystals in the rock types

Concerning the prevalence rate of the zircon morphology types in rock forming minerals, about 90% of short prismatic zircons was found to be embedded in biotite, normal zircons were present in about equal proportion in biotite and feldspar, and in much less frequently in amphibole, while long prismatic zircons were found to be typically hosted by felsic components, feldspar and quartz. The average size of zircon crystals is a critical factor when searching for 23 µm sized "homogeneous" areas for the LA spots. The characteristic sizes of the zircons both in the granitoids and in the mafic enclaves (ca. 200 µm and 50 to 150 µm, respectively) allow placing the analytical spots in intact areas having no inclusion (Nutman et al. 2014; Bell et al. 2018) or fissure and yielding quasi-homogenous CL pattern.

Internal textures of the zircon crystals

Normal and short prismatic zircon crystals show complex internal texture patterns in all the three sets of samples (Fig. 4). Long prismatic zircons possess minimal internal texture, if any. Primary texture types (Hanchar and Miller 1993), growth zoning (± antecrystic/xenocrystic core) and sector zoning, occur in all rock types.

Antecrystic/xenocrystic cores dominate the short prismatic crystals, but are present also in normal zircons. Two types of antecrystic/xenocrystic cores could be identified via their textural pattern. The first type is compact, containing neither thorite inclusions, nor spongy holes, although irregular, patchy-zoning texture is common (Fig. 4). The external border of these cores, which serves as template for the zircon overgrowth before and during the main magmatic crystallization event, is corroded. That type of core usually met the requirements set for selecting the analytical spots for geochronology. The other core type contains thorite inclusions and beyond them also spongy holes which have the same textural position, size and shape as the thorite inclusions. That thorite bearing ± "spongy" texture core can be found mainly in the mafic enclaves, less frequently in the host granitoid and does not appear in the hybrid rock. That second core type was excluded from the current dating because its structural state values typically exceeded considerably our cut off limit (< 18 cm^{-1}) for geochronology.

Secondary texture (Hanchar and Miller 1993), convolute zoning is common (~ 10%) in zircons of all three Mórágy rock types (Fig. 4).

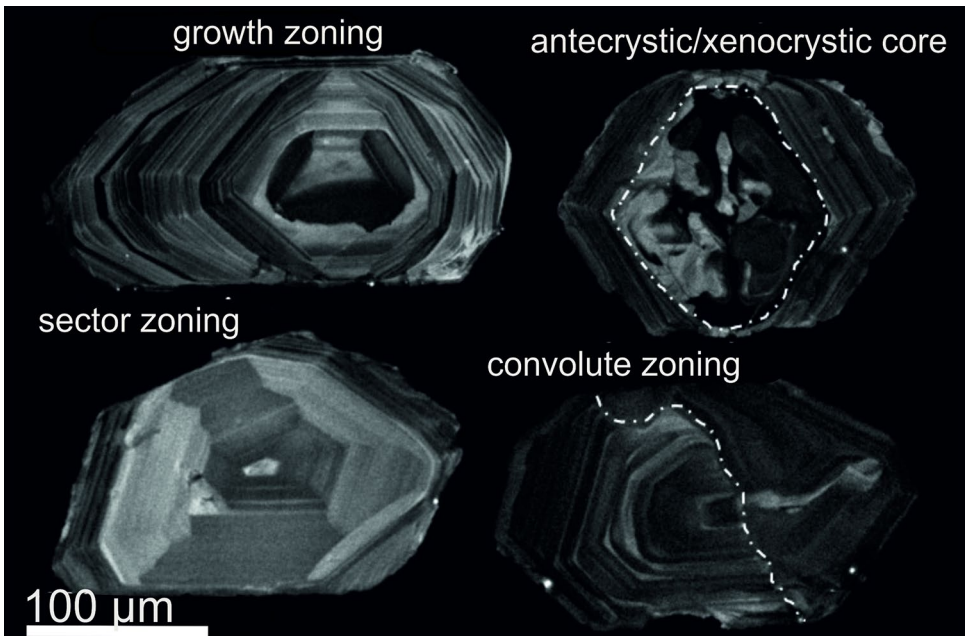

Fig. 4 Typical internal texture patterns of zircon crystals from the Mórágy intrusion: growth zoning, antecrystic/xenocrystic core (with patchy-zoning), sector zoning, convolute zoning

Structural state of the zircon crystals

Zircons from Mórágy and all rock types are predominately characterized by intermediate radiation damage densities, i.e. the FWHM of the ν_3 (SiO_4) Raman band (Murakami et al. 1986; Woodhead et al. 1991; Woensdregt 1992; Ellsworth et al. 1994; Nasdala et al. 1995, 1998; Zhang et al. 2000; Nasdala et al. 2001; Zhang and Salje 2001) values between 5 cm^{-1} and 15 cm^{-1}. Normal (Fig. 5a) and short (Fig. 5b) prismatic zircon crystals show zones of all structural states between 5 cm^{-1} and 25 cm^{-1}, while the metamict state (> 15 cm^{-1}) is not present in long prismatic zircon crystals (Fig. 5b).

U–Pb age data

Three hundred fifty preselected spots representing all the zircon morphologies and the key internal textural features of the three Mórágy rocks were analyzed by LA-ICP-MS in three sessions. The first session's setting was optimized for geochronology, the others for geochemistry. The full set of raw data is shown in the Electronic Appendix (Tables_S1 and S2). The U–Pb ages (Fig. 6) were grouped into three categories according to their discordance, based on Discordant I. data (Mezger and Krogstad 1997; Nemchin and Cawood 2005): 1) concordant ages (< 10% discordance, one hundred eighty data; out of which only three had no intersection with the concordia curve) 2) slightly discordant ages (10–17% discordance, twenty-six data, out of which no one intersects the concordia curve), 3) strongly discordant ages (> 17% discordance, sixty-four data). It has been previously emphasised that age data span obtained from zircon grains can be interpreted as representatives of the whole timespan of crystallization (von Quadt et al. 2011; Wotzlaw et al. 2013).

We processed only the concordant and slightly discordant ages. The 17% maximum discordance threshold was set based on the mean square weighted deviation (MSWD) value: at that discordance the MSWD (2.3) value was still acceptable, hence interpretable lower intercept ages could also be taken into account.

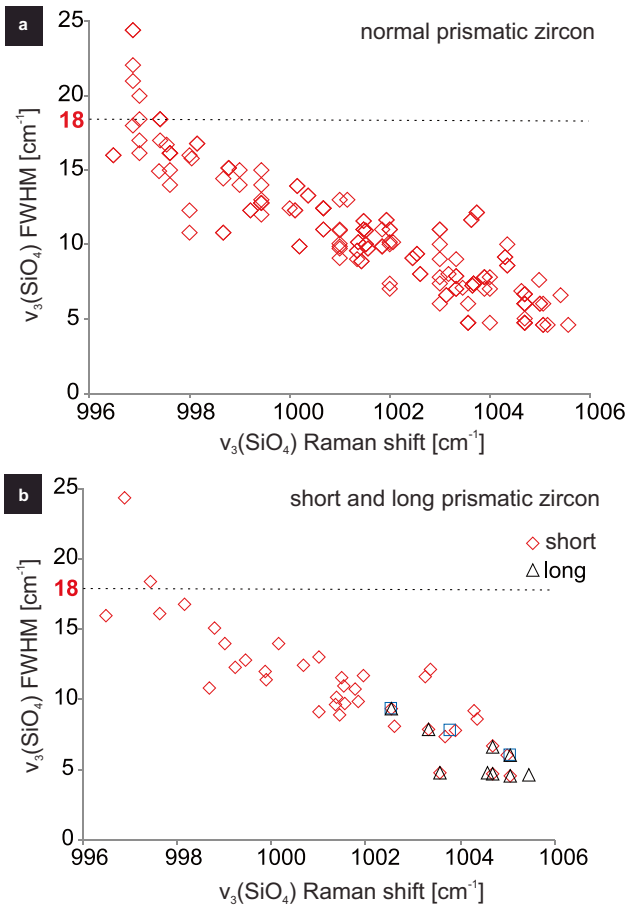

Fig. 5 Structural state of the Mórágy zircon crystals by morphology types, characterized by the position of the ν_3 Raman peak vs. full width at half maximum (FWHM) values (Nasdala et al. 1995, 1998). Horizontal dotted line: cut off value (18 cm^{-1}) of the current study for age determination

Concordant ages

The bulk of the one hundred eighty concordant U–Pb data (Table 1, Table S1), in one hundred nine zircon grains fall in the 290–370 Ma time interval, but most of data falls between 310–360 Ma. Based on main rock type (granitoid), the data sets (Fig. 7a, b) define a concordia age of 339.2 ± 4 Ma (MSWD = 1). The two other rock types (hybrid, mafic enclave) in Mórágy show a concordia age of 339.6 ± 4 Ma (MSWD = 1.4).

Although the pluton yield concordia ages, the great differences in single-spot ages (Fig. 7a, b) indicate the potentially multimodal character of the age distribution for all rock types. The calculated histogram using UNMIX algorithm shows partly overlapping curves (Fig. 8). t-test (Pearson 1939), however confirmed (< 0.5) the presence of two statistically separable age components The actual age value pairs: 347.2 ± 1.1 Ma and 333.5 ± 1 Ma (granitoid), 344.8 ± 2.5 Ma and 333.4 ± 1.5 Ma (hybrid rock) and 343.7 ± 1.3 Ma and 332.1 ± 2 Ma (mafic enclave).

Concordant age data distributions showed no variations (within error) when tested by grouping the zircon grains analyzed regarding their external morphology or internal texture types. For external morphology, however, it is worth mentioning that the bulk of the concordant ages belong to normal prismatic crystals, also long prismatic type is mostly concordant, while the short type both in the granitoid and mafic rock are practically missing from the concordant group. The latter is a simple result of the textural situation: short zircons are dominated by the antecrystic/xenocrystic core for volume and the narrow growth rim is normally not wide enough (< 20 μm) for positioning an undisturbed LA analytical spot.

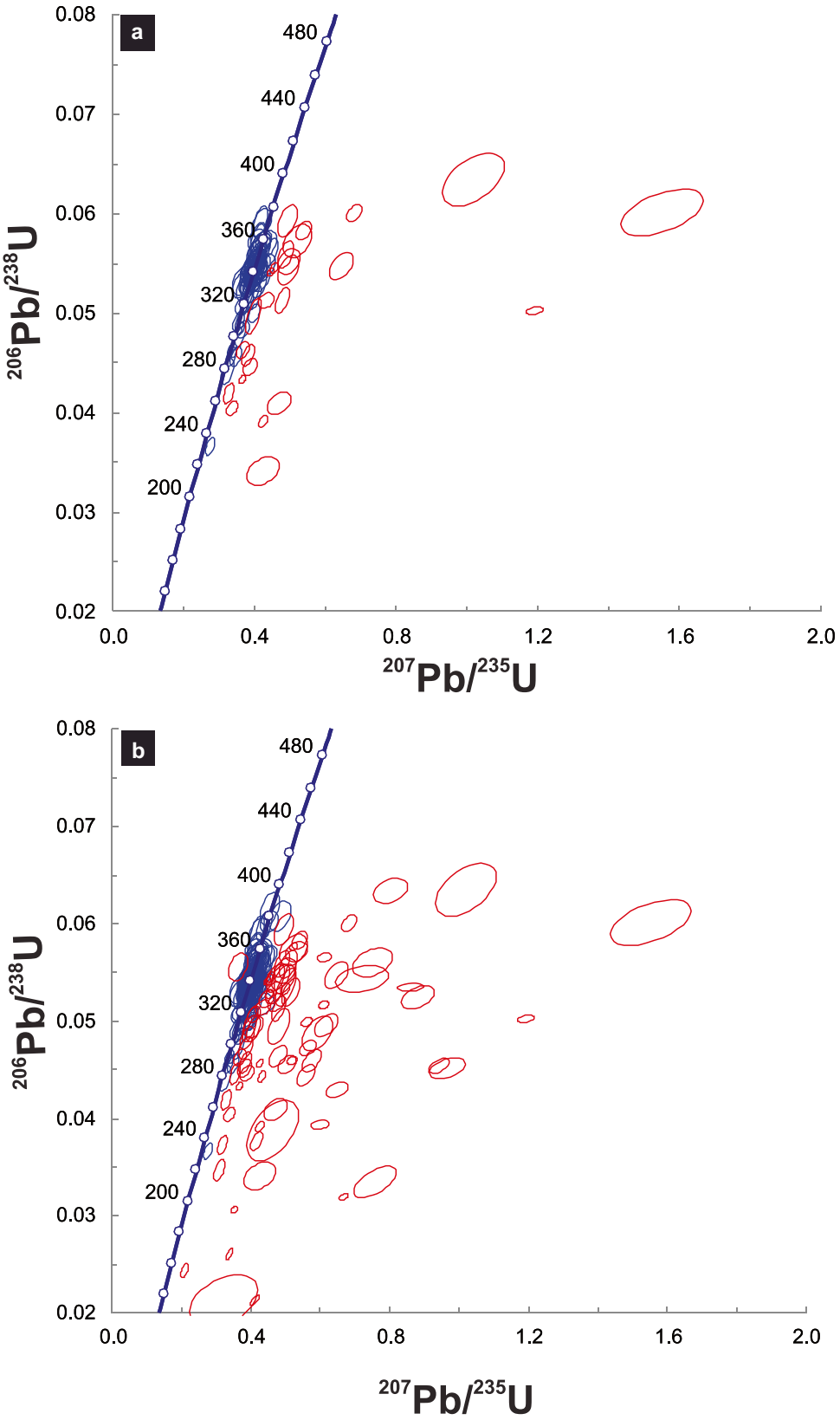

Fig. 6 **a**, **b** The complete set of measured zircon age data plotted by rock types: a) Granitoid: Mórágy; and b) Hybrid + mafic rock Mórágy (n = 5 data is outside of the plotted range). Blue ellipses represent the concordant (± 10%), red the discordant I. (> 10%) data

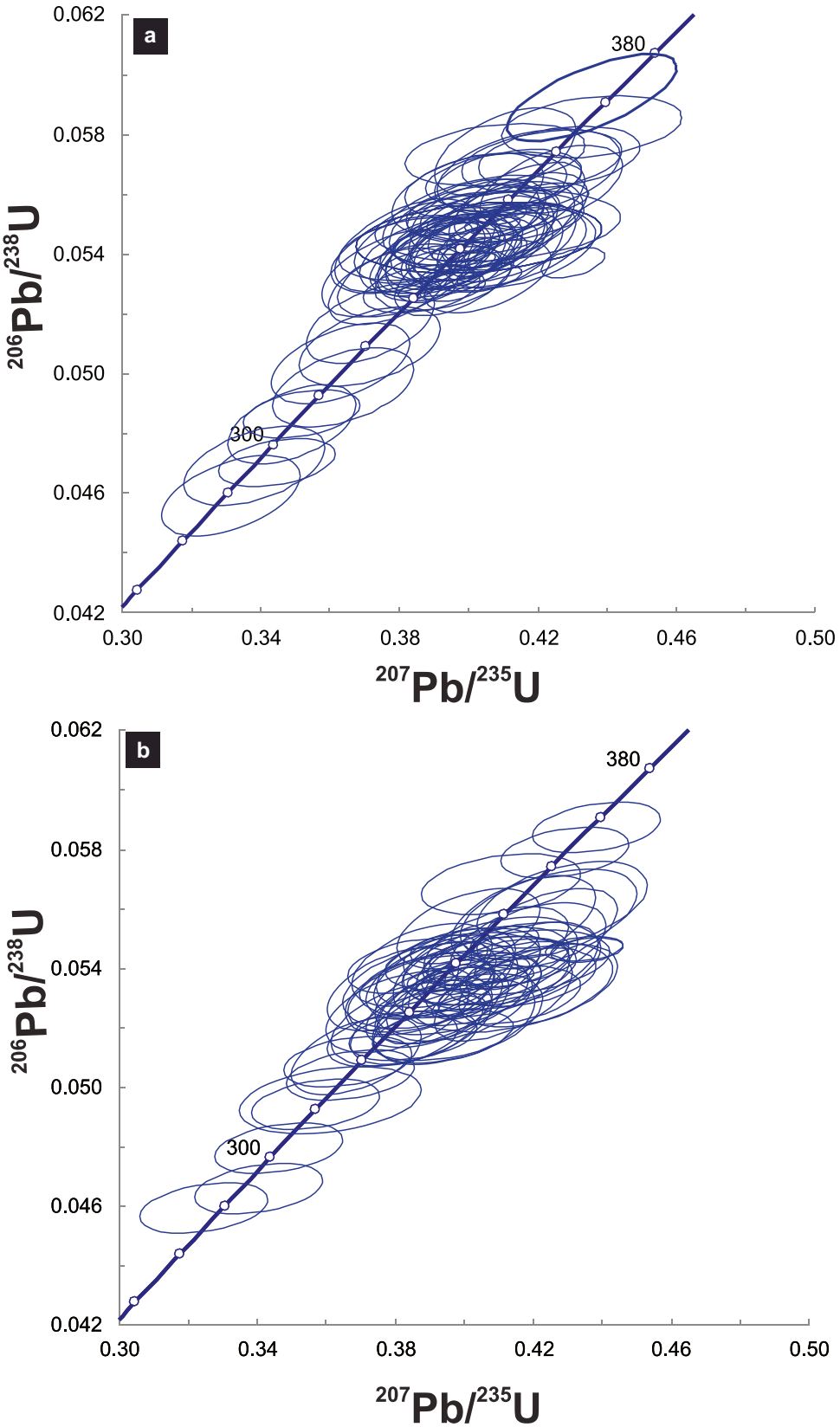

Fig. 7 **a**, **b** Concordant (< 10% discordance) zircon age data plots of Mórágy pluton by rock types. Concordia U–Pb age (370–290 Ma) of all three rock types from Mórágy. Granitoid: **a**) (339.2 ± 4 Ma MSWD = 1); Hybrid + mafic rock: **b**) (339.6 ± 4 Ma MSWD = 1.4). Blue ellipses represent the concordant (± 10%)

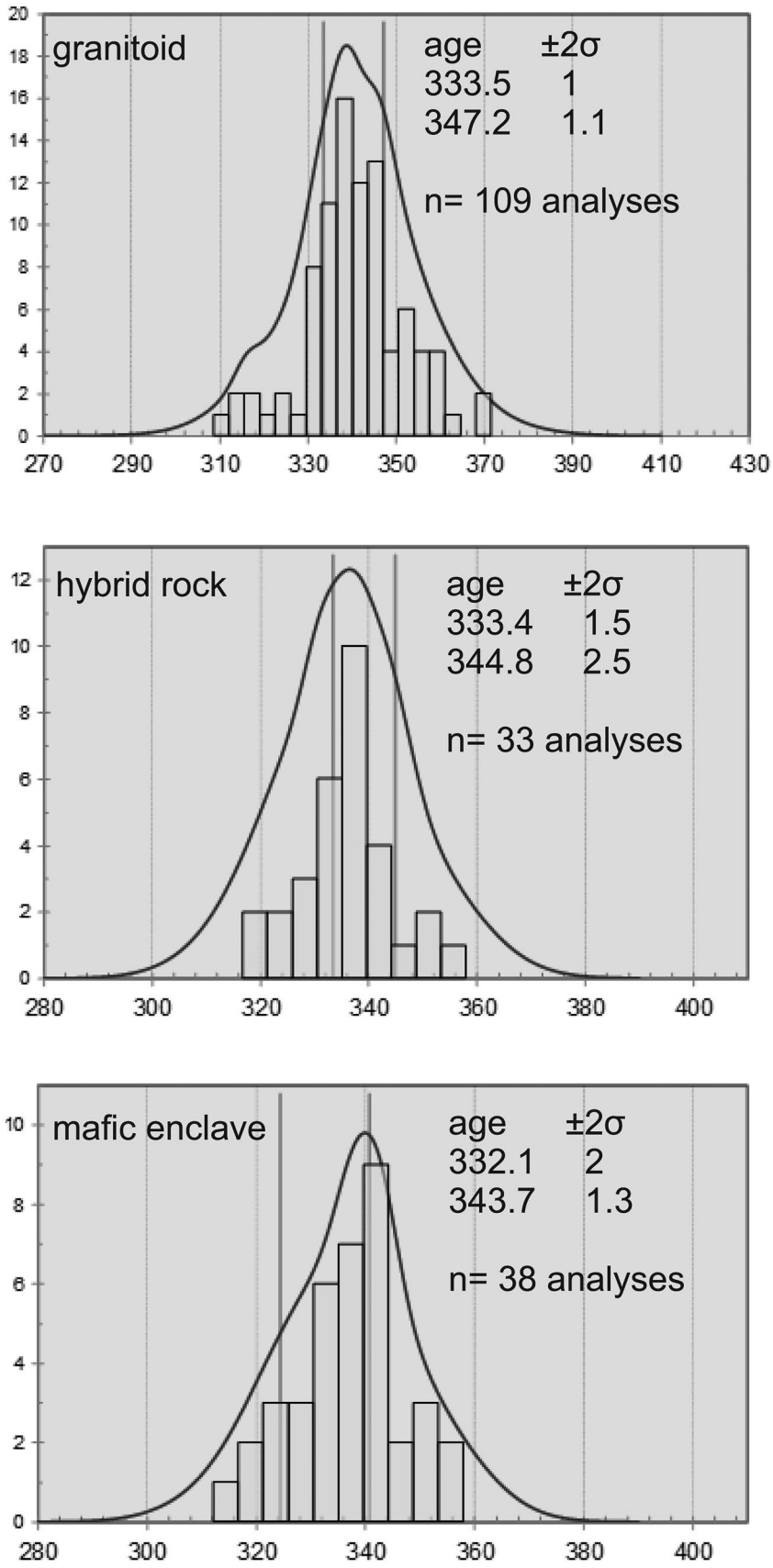

Fig. 8 Bimodal distribution of the 360 – 310 Ma age range concordant age data by rock types from Mórágy

Discordant ages

Ninety discordant ages concern the three rocks, with a clear dominance of the mafic enclave. The only systematic connection found between the discordant ages and the zircon external morphology and/or internal texture was that short prismatic cores gave discordant ages.

Slightly discordant ages

Twenty-six analyses are slightly discordant (Table_S2). The linear regression (Fig. 9a, b) yields lower intercept age 114 ± 25 Ma (MSWD = 2) for the granitoid, 115 ± 48 Ma (MSWD = 2.3) for the hybrid and mafic enclave rocks.

Highly discordant ages

Sixty-four analyses are highly discordant, falling in the 18–35% discordance range (the data set is available in Table S2). 64 is the number of highly discordant U–Pb data. This data set was obtained from the measurements of 23 zircon grains, from which 5 were in granitoids, and 18 were in hybrid rocks and enclaves together. They represent predominantly zircon antecrystic/xenocrystic cores in the mafic rock, with a clear dominancy of short prismatic morphology over normal prismatic. From the point of view of structural state most of the highly discordant ages belong to metamict or upper zone intermediate (> 12 cm^{-1} FWHM) structural group areas (Fig. 5a, b). Our present paper does not attempt to interpret geologically these highly discordant data.

Concordant ages in terms of zircon internal texture patterns

Normal and short prismatic zircon crystals characterized only by primary type internal structure show heterogeneous internal age distribution. In most cases the age distribution pattern could not be interpreted directly, e.g. core and outermost rim is of the same older age, whereas the part in between is of younger age (Fig. 10a). Similar trends were formerly reported from several sites, including Australian (Pidgeon et al. 1998) or Canadian granitoids (Van Lankvelt et al. 2016). There was, however, a connection between the age pattern and the structural state pattern of the crystals: the younger ages, for the most part was found in crystal areas of worse structural states. The typical structural state difference between areas showing significant age differences was > 3 cm^{-1} FWHM of the ν_3 (SiO_4) Raman band (Fig. 10a). In some cases, the age distribution pattern itself showed a logical trend, older age being in the core and subsequently younger ones towards the rim, however in all of these cases the structural state pattern showed also a parallel worsening (Fig. 10b). No crystals with younger rim and older core were found having the same/similar structural state. Very rarely (in the case of just two short prismatic crystals), however, we found no age difference between crystal areas of different structural states (Fig. 10c).

Secondary texture (convolute zoning) areas show always ages much younger than the primary texture related areas, but better structural state (Fig. 10d) can be observed. In contrast to the normal and short morphological types, in the case of long prismatic zircon crystals age inhomogeneity is present without internal variation of structural state, hence there is no obvious BSE contrast, yet CL images demonstrate the presence of internal texture even in these cases (Fig. 10e).

Titanium content of zircon crystals

The geochemistry optimized setting of the LA-ICP-MS data collection gave information also about the Ti content of zircons. Ti concentrations, one hundred nine data varying from 1 to 32 ppm, are summarized in Table S3.

Discussion

Presence and age of pre-Carboniferous antecrystic/xenocrystic cores in zircons

There is ample evidence for older than Variscan zircon ages from all over the Bohemian Massif (Grauert et al. 1973; van Breemen et al. 1982; Zwart 1986; Kröner et al. 1988; Zoubek 1988; Gebauer et al. 1989; Wendt et al. 1993; Klötzli et al. 2004; Žák et al. 2014), proving that heterogeneous Proterozoic crust was reworked into the Variscan realm in Central Europe.

Our concordant age data collected on one of the two antecrystic/xenocrystic core types, the thorite-free antecrysts/xenocrysts however remain within the Carboniferous age. The seeming contradiction between the pre-dating textural position and with the magmatic event synchronous radiometric age can be dealt with assuming a complete, temperature-based reset of the zircon U–Pb isotope system of these cores during the main magmatic event (mantle source of Durbachite plutons) in Carboniferous at the latest (Clemens 2014).

On the other hand, *qualitatively* we are able to confirm the existence of inherited, likely pre-Variscan zircon antecrystals/xenocrystals in the Variscan magma. These antecrystic/xenocrystic cores dominate the short

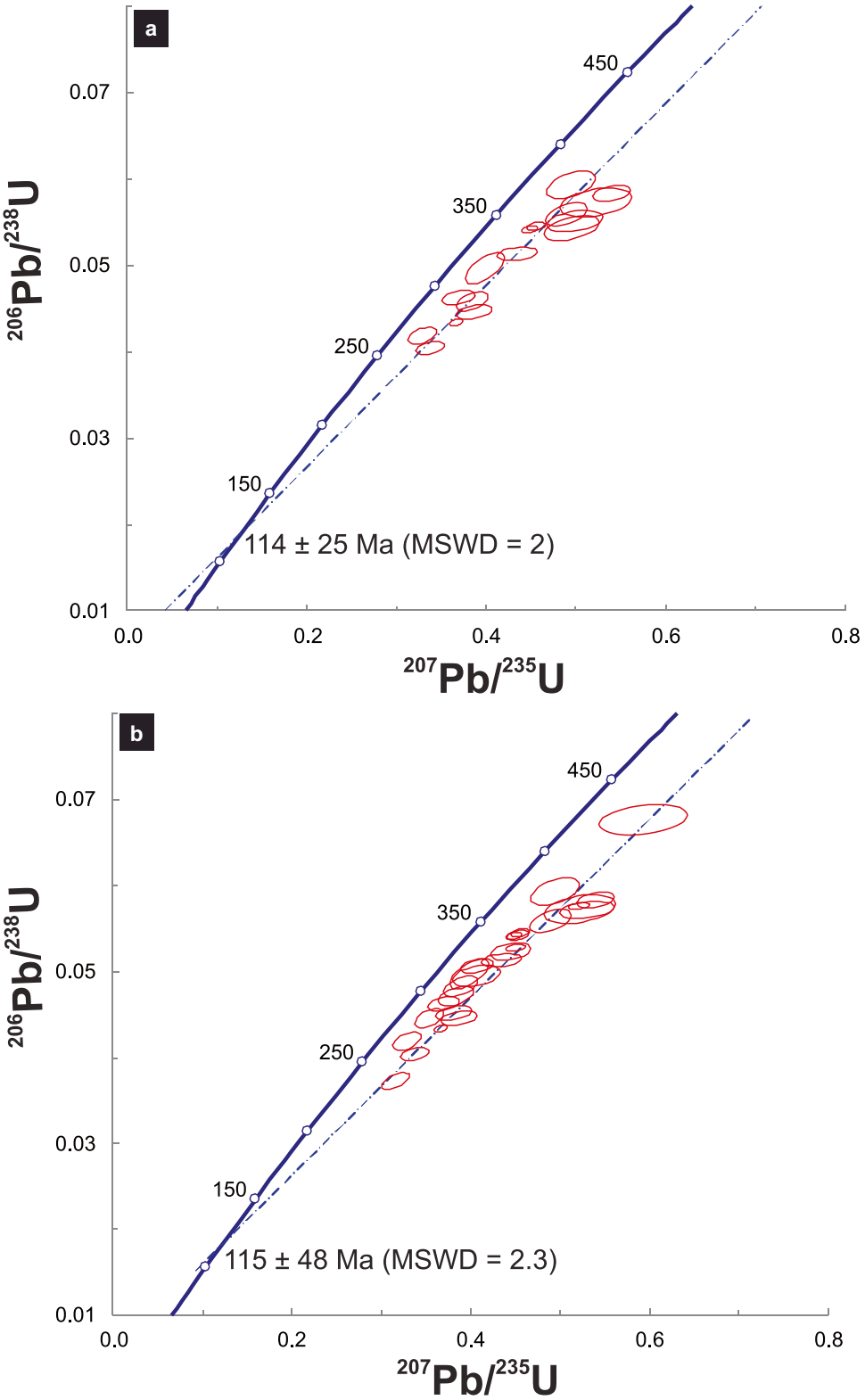

Fig. 9 **a**, **b** Slightly discordant (10%-17%) age data with calculated lower intercepts by rock types from Mórágy, **a**) granitoid, lower intercept age 114 ± 25 Ma (MSWD = 2), **b**) hybrid + mafic enclave, lower intercept age 115 ± 48 Ma (MSWD = 2.3). Red ellipses represent the discordant I. (> 10%) data

prismatic zircons. Mainly biotite, the first crystallizing rock forming mineral captures these zircons. The narrow magmatic growth rims of short prismatic zircons indicate a relatively short time between the start of biotite crystallization and encapsulation and/or low zirconium oversaturation of magma.

The missing pre-Carboniferous core ages do not necessarily contradict the older age data previously reported for Mórágy (Klötzli et al. 2004), as that former study did not document and interpret its data in terms of concordance and direct textural position. In our present paper the second type, thorite-bearing antecrystic/xenocrystic cores were excluded from the age determination on grounds of their strong metamict structural state. We assume that those old radiometric ages in Mórágy, would be strongly discordant, hence their direct, geological interpretation would be difficult. An open question, however still remains: why and how could these assumed older zircon crystals avoid the temperature driven isotope diffusion in melt conditions while others could not? Further, more direct analysis of the thorite-bearing antecrystic/xenocrystic cores may offer answers and a deeper insight into of the origin of the magmas, too.

Ti in zircon geothermometry

The Ti-in-zircon thermometer to granitic rocks is based on the Si replacement by Ti in the crystal structure (Cherniak et al. 1997a, Harrison et al. 2005; Szymanowski et al. 2018). According to Watson et al. (2006), the inherent incompatibility of Ti in zircon leads to expected. Ti concentrations in the 0.3–50 ppm range under most circumstances correspond to 500 °C – 900 °C magma temperature. The experiments define a log-linear dependence of equilibrium Ti content (expressed in ppm by weight) upon reciprocal temperature: $T(^{\circ}C)zircon = \frac{5080\pm30}{(6.01\pm0.03)-\log(Ti)} - 273$ (Watson et al. 2006). Ti-in-zircon thermometry could achieve the capability to determine the magma temperature of granites with uncertainty as low as approximately ± 20–30 °C (Schiller and Finger 2019).

Our data (Table S3) varying from 32 to 1 ppm correspond to Ti-in-zircon temperatures of 854–552 °C. The calculated data come from mainly normal prismatic zircon crystals (91). The rest consists of the short prismatic (2) and long prismatic zircon crystals (16).

For a normal prismatic zircon crystal, the Ti concentrations cover a wide range from 27 to 1 ppm, indicating the Ti-in-zircon temperatures 836–552 °C. This result proves that they are presented throughout the whole-time interval of the granitic magma crystallization.

Furthermore, the Ti concentration with the Ti-in-zircon temperatures are decreasing from the zircon's (antecrystic/xenocrystic) core (26–7 ppm, 832–711 °C) to the (growth zoning) rim (16–1 ppm, 783–552 °C). It has to be noted, that there are no any differences in Ti concentrations data between the simple core (center of crystals) and antecrystic/xenocrystic core of normal and short prismatic zircon crystals. In the case of long and short prismatic zircon crystals, the Ti values are between 32–8 ppm, showing the upper-temperature range (854–719 °C) (Fig. 11).

Interpretation of concordant age data

Mórágy primary magmatic rock types: age and genetic relationship

The U–Pb concordia age of zircons from the Mórágy main rock type, the host granitoid is 339.2 ± 4 Ma (MSWD = 1). This age is not in contradiction with the zircon U–Pb age reported by Koroknai et al. (2010) and the younger age of Klötzli et al. (2004), measured on separated short prismatic zircons only (Fig. 3). Our present age data, however, in contrast to the observations of Klötzli et al. (2004), does not uphold an age difference between the different zircon external morphology types. The concordia age was invariant for the zircon morphology, the calculated age is based on overall data from all morphology types.

The large number (hundred-nine) of individual concordant zircon age data in the 360–310 Ma time interval from the granitoid rock (Fig. 7a, b) allowed us to reveal the bimodal distribution of the data showing two maxima (347.2 ± 1.1 Ma and 333.5 ± 1 Ma; see Fig. 8). The bimodality in the age distribution has no connection with zircon morphology.

In the case of the mafic enclave (forty-three concordant analyses) and hybrid rock (thirty-eighty concordant analyses) of Mórágy both concordia age (343.7 ± 1.3 Ma resp. 332.1 ± 2 Ma (MSWD = 1.4, MSWD = 1.2) and the bimodality, including the particular maximum ages (Fig. 8) fit the granitoid data within error, or very closely. Again, no connection could be found between age data and external morphology type of the zircons.

The good fit between the granitoid and the mafic enclave magmatic crystallization zircon ages gives a geochronological proof for the simultaneous presence of two coexisting magmas, suggested by Király and Koroknai (2004) based on petrological and geochemical observations. In our view the size scale of the mafic enclaves (dm–m) indicates magma mingling (Kuşcu and Floyd 2001; Baxter and Feely 2002; Ventura et al. 2006) between the granitoid magma and the lamprophyre-derived mafic magma, while the hybrid rock can be put down to mixing (Foster and Hyndman 1990; Neves and Vauchez 1995; Johnson and Barnes 2006; Peytcheva et al. 2008; von Quadt et al. 2014) of the two magmas in their narrow contact zone.

The age distribution of the mafic enclave zircons, however, differs from that of the granitoid, being the first

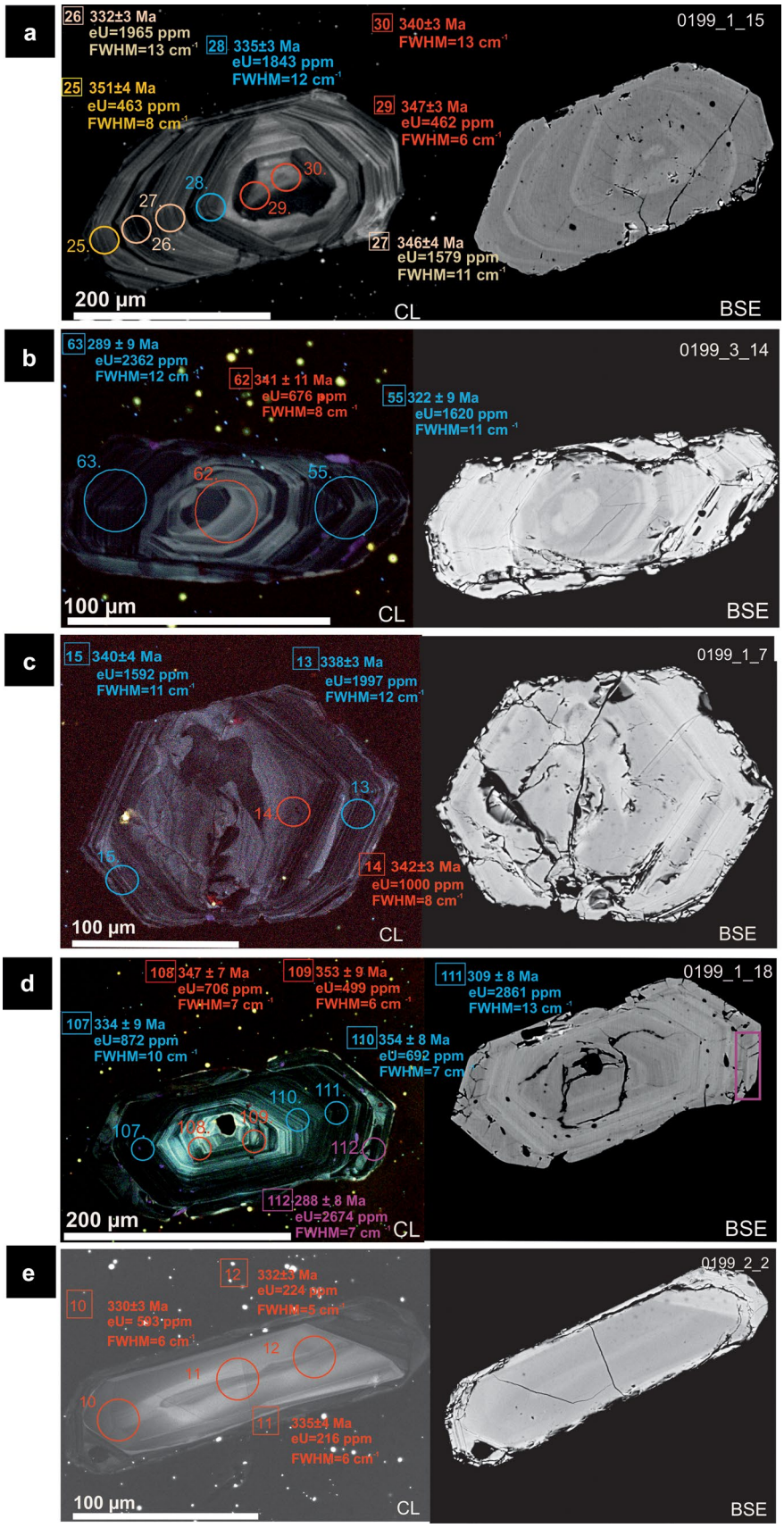
a
26 332±3 Ma
eU=1965 ppm
FWHM=13 cm-1
28 335±3 Ma
eU=1843 ppm
FWHM=12 cm-1
25 351±4 Ma
eU=463 ppm
FWHM=8 cm-1
30 340±3 Ma
FWHM=13 cm-1
29 347±3 Ma
eU=462 ppm
FWHM=6 cm-1
27 346±4 Ma
eU=1579 ppm
FWHM=11 cm-1
0199_1_15
200 µm
CL
BSE
b
63 289 ± 9 Ma
eU=2362 ppm
FWHM=12 cm-1
62 341 ± 11 Ma
eU=676 ppm
FWHM=8 cm-1
55 322 ± 9 Ma
eU=1620 ppm
FWHM=11 cm-1
0199_3_14
100 µm
CL
BSE
c
15 340±4 Ma
eU=1592 ppm
FWHM=11 cm-1
13 338±3 Ma
eU=1997 ppm
FWHM=12 cm-1
14 342±3 Ma
eU=1000 ppm
FWHM=8 cm-1
0199_1_7
100 µm
CL
BSE
d
108 347 ± 7 Ma
eU=706 ppm
FWHM=7 cm-1
109 353 ± 9 Ma
eU=499 ppm
FWHM=6 cm-1
107 334 ± 9 Ma
eU=872 ppm
FWHM=10 cm-1
110 354 ± 8 Ma
eU=692 ppm
FWHM=7 cm-1
111 309 ± 8 Ma
eU=2861 ppm
FWHM=13 cm-1
112 288 ± 8 Ma
eU=2674 ppm
FWHM=7 cm-1
0199_1_18
200 µm
CL
BSE
e
12 332±3 Ma
eU=224 ppm
FWHM=5 cm-1
10 330±3 Ma
eU=503 ppm
FWHM=6 cm-1
11 335±4 Ma
eU=216 ppm
FWHM=6 cm-1
0199_2_2
100 µm
CL
BSE

◂**Fig. 10** **a** Normal prismatic zircon (grain #0199_1_15) with growth zoning texture. SEM-CL and SEM-BSE image pairs. Circles show the U–Pb dated areas, numbers refer to the zircon analysis ID (#25–30) of the given areas. Same color means the same internal texture part. Concordant age with error (Ma), effective U=eU(ppm)=U(ppm)+0.24*Th(ppm) and ν_3 (SiO_4) FWHM (cm^{-1}) are indicated to each area analyzed; **b**: Normal prismatic zircon (grain #0199_3_14) with growth zoning texture. SEM-CL and SEM-BSE image pairs. Circles show the U–Pb dated areas, numbers refer to the zircon analysis ID (#55, 62– 63) of the given areas. Same color means the same internal texture part. Concordant age with error (Ma), eU (ppm) and ν_3 (SiO_4) FWHM (cm^{-1}) are indicated to each area analyzed; **c**: in Short prismatic zircon (grain #0199_1_7) with growth zoning texture over a large antecrystic/xenocrystic core showing irregular, patchy-zoning texture. SEM-CL and SEM-BSE image pairs. Circles show the U–Pb dated areas, numbers refer to the zircon analysis ID (#13–15) of the given areas. Same color means the same internal texture part. Concordant age with error (Ma), eU (ppm) and ν_3 (SiO_4) FWHM (cm^{-1}) are indicated to each area analyzed; **d**: Normal prismatic zircon (grain #0199_1_18) with growth zoning and convolute zoning (outermost rim) textures. SEM-CL and SEM-BSE image pairs. Circles show the U–Pb dated areas, numbers refer to the zircon analysis ID (#107–111) of the given areas. Same color means the same internal texture part. Concordant age with error (Ma), eU (ppm) and ν_3 (SiO_4) FWHM (cm^{-1}) are indicated to each area analyzed; **e**: Long prismatic zircon (grain #0199_2_2) with weak irregular internal texture. SEM-CL and SEM-BSE image pairs. Circles show the U–Pb dated areas, numbers refer to the zircon analysis ID (#10–12) of the given areas. Concordant age with error (Ma), eU (ppm) and ν_3 (SiO_4) FWHM (cm^{-1}) are indicated to each area analyzed

maximum (~ 344 Ma) the dominant, while in the case of the hybrid rock a balanced frequency of the two age populations can be seen (Fig. 8). These distributions are challenging for geological interpretation, but no model was found to describe the evolution of the system in terms of different rock types giving similar distributions.

Post magmatic event reflected in the slightly discordant zircon ages

The lower intercept age of the granitoid and the two other rock types from Mórágy is Cretaceous (114 ± 25 Ma; 115 ± 48 Ma). The Cretaceous overprint of the Mórágy Hill rocks can be put down to the alkaline basalt volcanism of the Mecsek Mts. (Haas et al. 2014), most active in the 135–100 Ma period (Harangi and Árváné Sós 1993). That extension-related alkaline magmatism was the consequence of the detachment of the Tisza Mega-unit from the European Plate during the Tethyan rifting.

Zircon internal texture patterns confronting statistical interpretation of concordant age data

The above presented analysis, based on solely statistical interpretation of a large number of properly controlled concordant U–Pb age data, gave a picture that conforms to the large-scale tableau of the evolution of granitoids. Geochronology based indication of several million years long crystallization is no novelty. For example the Half Dome pluton in Yosemite National Park was assembled over a period of at least 10 Ma, between 95 and 85 Ma, and that the Half Dome Granodiorite intruded over a period approaching 4 Ma

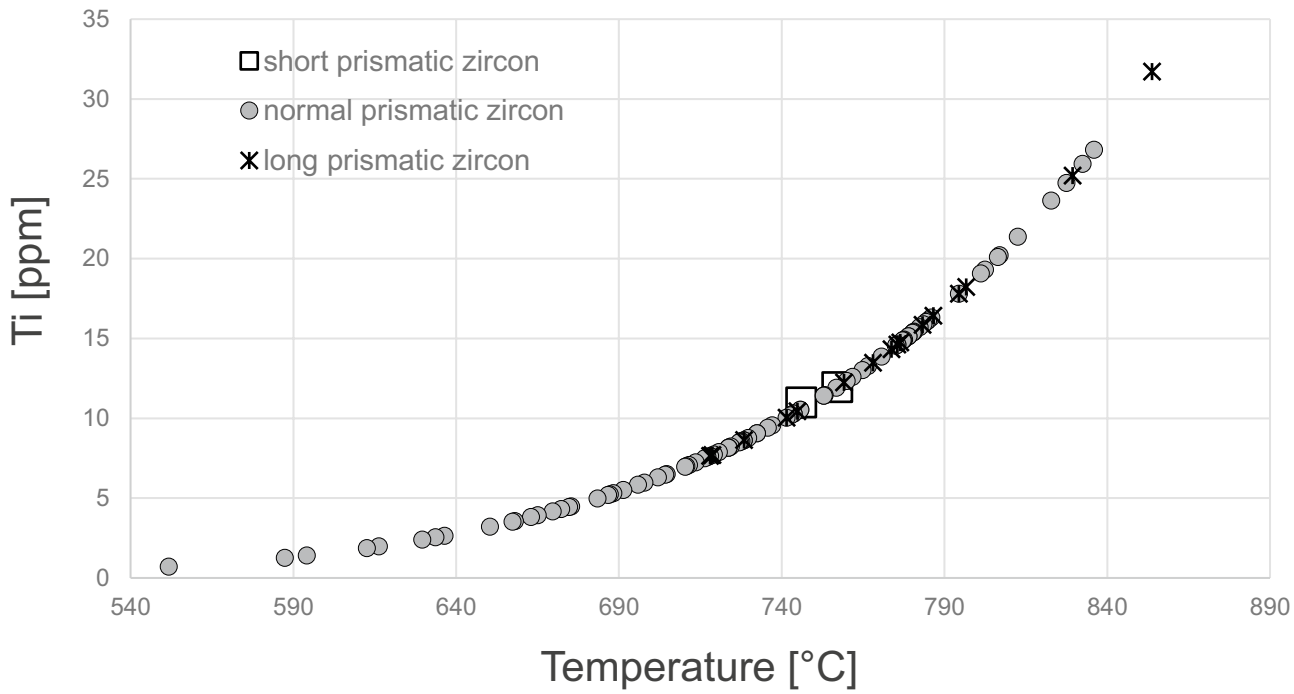

Fig. 11 Ti concentration in the different morphological types (short, normal, long) of zircon crystals

(Coleman et al. 2004). Such processes can be explained by simple thermal models demonstrating the need of a series of magma injection pulses over a several Ma time span into the large plutons cooling solely by conduction (Coleman et al. 2004). For Mórágy Király and Koroknai (2004) likewise puts forward a multiple injection, heterogeneous magma model when discussing the importance of mixing (mingling) processes in the generation of these rocks.

On the other hand, if our concordant age data are treated not simply on a statistical base, but are analyzed in local context in terms of internal texture of the zircon crystals, the picture becomes controversial. Moreover, the small, less than hundred meters scale of borehole sampling in the current study makes it also difficult to explain the presence of zircons formed at different times in separately intruded larger scale magma body.

The statistically proved bimodality, if real, would indicate a space and/or time separated distribution of the data sources, the LA-spots analysed. Space separation would mean some kind of separation of two sets of zircon grains, one carrying basically "older" (~345 Ma), the other "younger" (~335 Ma) ages. Time separation could be directly traced if age data within one crystal would get consequently younger from core to rim. This feature is not unique since previous works have found that the core and the rim gave different U ages (Van Lankvelt et al. 2016). It is also necessary to mention that the U concentrations in the cores and rim zones of zircon grains are usually different, as it was described by Pidgeon et al. (1998), Marsellos and Garver (2010).

None of the two cases outlined above apply to our data set. True that there are zircons relating to basically just one narrow age interval (Fig. 10c), but these "single" ages do not concentrate around the calculated "older" and "younger" maxima, their distribution is arbitrary within the whole period. True also that in some zircons younger ages from core to rim are apparent (Fig. 10b), others, however, are also "old" both at the core and at the outermost rim, and younger in between (Fig. 10a).

These observations urge us to reconsider the validity of our geological model made up following the traditional data interpretation paths. When searching for other models we examined, among others, the potential connection between the structural state and the measured concordant age of the individual LA-spots (Fig. 12). The graph shows qualitatively that the highest age group of the normal and short prismatic zircons (~355 Ma) is connected to the least disturbed structural states (ν_3 FWHM: 6–8 cm^{-1}). Going back to the local, single grain scale a similar tendency can also be observed (Figs. 10a, b).

A combined approach for interpreting the overprinted zircon age set

Assuming several Variscan magma intrusion pulses, in a combined model only short periods of > 10 Ma can be identified based on concordant U–Pb ages.

We have found that Variscan zircon U–Pb isotope system closed at 350 Ma and later suffered a Permian (~270 Ma) overprint. This latter one caused lead loss of 90–10%; however, the data remain still concordant, and the apparent ages got younger by 10–5 Ma.

If this model were valid, then our long, practically continuous set of measured 'magma crystallization' zircon ages would only reflect the slight local differences of structural state in zircon at the time of the overprinting effect. Clearly, in that extreme of the model the age bimodality would mean only, that there was a bimodality in the structural state of zircons when overprinted. Such a structural state bimodality could finally be connected to a pulsing multimodality of magma reflected in changing built in U, Th content during the crystallization of zircon crystals before they got captured by the co-crystallizing rock forming minerals. The documented strong growth zoning may also contribute to that condition.

In this model we cannot give the real formation age of the system, as we cannot prove that the members of the oldest measured larger age set (~355 Ma) haven't suffered any lead loss. Accordingly, that ~355 ± 3 Ma age could be regarded as minimum age, possibly not far from the real age of magma cooling below the zircon U–Pb closure temperature (Lee et al. 1997; Cherniak and Watson 2001; von Quadt et al. 2014).

Further age refinement may be hoped if we collect more data on the relatively rare long prismatic zircons. They are of the best structural state (5–6 cm^{-1}, Fig. 12), carrying potentially the least disturbed isotope age information. Those morphology type zircons may play a key role in understanding the complicated magmatic- and post-emplacement thermal history. In that respect the strong concentration of the long prismatic concordant zircon ages (apart from the cores) around 334 ± 3 Ma (Fig. 12) may carry the message that the system crossed the ~650 °C isotherm at that time.

Reconstruction of the major events of the development of Mórágy pluton according the zircon U–Pb age constraints

Our observations permit us to set up a five step zircon geochronology-based model for the magmatic evolution of the studied granitoids (phases A–E), followed by a post-magmatic event (phase F). In the first phase (phase A) two magmas, a granitoid felsic and a lamprophyre-derived mafic were generated separately. Both melts might have contain partially resorbed,relict zircon crystals (± thorite), evidence that the melts were undersaturated for Zr at the time of their formation.

Later, in phase B, probably above the zircon U–Pb closure temperature, the melts became oversaturated for zirconium and slow crystallization of zircon started in the melts. The corroded relict zircon crystals acted as seedings, but

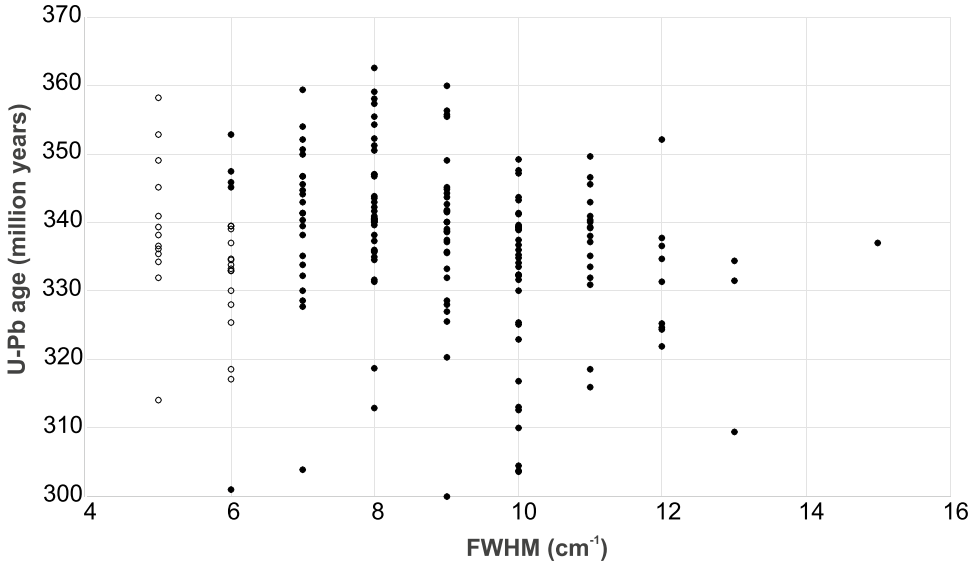

Fig. 12 Concordant U–Pb age (Ma) plotted against the structural state (ν_3 (SiO_4) FWHM; cm^{-1}) of the individual LA-spots analyzed by zircon morphology types. Circles: long prismatic zircons, dots: normal and short prismatic zircons

the formation of new zircon crystals started, too. In phase B the thermodynamic conditions favored the long and short prismatic type zircon growth morphology over the normal prismatic type. At this phase, the two magmas remained within similar P–T conditions from the point of view of zircon crystallization.

By cooling of the system crystallization of rock forming minerals was initiated (phase C). The first dominant mineral, biotite, captured the bulk of short prismatic zircons dominant in the melt. At this phase the system passed the zircon U–Pb closure temperature range. This is the first point when we can try to assign time and temperature to the system (~ 800–850 °C; ~ 355 ± 3–4 Ma). For zircon crystal morphology the normal prismatic type gains dominance over the short and long types. Already at this phase, or at the beginning of the next (phase D) at the latest, mingling of the two magmas went on, and a single (in terms of space, time, P–T conditions), yet still two-component system came about. At the border zone of the two magmas the hybrid melt was generated by mixing.

Phase D, the further cooling resulted in the main crystallization of the three rock types. By the end of phase D only a very minor melt portion of the magmas remained. Zircon crystallized continuously in normal prismatic shape and is subsequently captured by the co-crystallizing rock forming minerals. The intensive growth zoning of zircon indicates slightly fluctuating temperature-concentration(-pressure?) conditions, a result of which is that higher or lower affinity of zircon structure for hosting U and Th. Phase D may overarch the 350–340 Ma period and the 800–700 °C temperature range, which is confirmed by Ti-in-zircon thermometry (Table S3).

Phase E is the eutectic crystallization of the rest magmas. Long prismatic zircon morphology turns up beside the still existing normal prismatic shape. The rims of these long and normal prismatic zircons are embedding Na-free K-feldspar, albite and quartz, indicating a ~ 650 °C closing temperature. The best (5–6 cm^{-1}) structural state long prismatic zircons show the ~ 334 ± 4 Ma closing age.

The post-crystallization history can be characterized by three, distinguishable events.

F1 event: Lead loss of worse structural state zircon zones results in younger concordant ages without destroying the growth zoning and without improving the structural state of zircon. That event brought about an inhomogeneous shift of some of the concordant U–Pb zircon ages towards the younger ages, a shift sometimes of only a few millions or several tens of millions of years. This is the reason for an unaccountable smearing of the crystallization age distribution curves.

F2 event: Convolute zoning fully overprints the former (primary) zircon internal texture by mobilizing elements (Putnis 2009), equalizing trace element concentrations and locally reconstructing the structural state of zircon (from ~ 12–13 cm^{-1} up to ~ 7–9 cm^{-1}). Though convolute zones give well defined concordant zircon U–Pb ages (~ 300 Ma).

F3 events: Overprints causing slightly discordant ages. Without knowing their mechanisms in detail the lower intercept age could be attributed well to the Cretaceous rift-related magmatism affecting the Mórágy basement.

Conclusions

Texture related U–Pb zircon geochronology shows that the Mórágy pluton has a complex magmatic and post-crystallization history. Based on a large set of zircon internal texture related LA-ICP-MS U–Pb age data obtained from carefully pre-screened

zircon crystals, a five step (phases A–E) zircon-centred model could be set up regarding the formation of the magmatic rocks outcropping at Mórágy Hills. The simultaneous long consolidation history of the two magmas, felsic and mafic, is typical for "durbachite-type" complexes.

We may conclude that our multiphase sample pre-selection protocol combined with a new complex age data interpretation model is promising for future zircon U–Pb geochronology of overprinted geological systems.

Supplementary Information The online version contains supplementary material available at https://doi.org/10.1007/s00710-023-00817-2.

Acknowledgements We express our thanks for a CEEPUS scholarship supporting the field work in Austria. We are indebted to Professor Urs S. Klötzli for the lab work, to ELTE Faculty of Science Research and Instrument Core Facility for the access to the Raman laboratory. Supported By the ÚNKP (1783-3 / 2018 / FEKUTSRAT) New National Excellence Program of the Ministry of Human Capacities. We thank GÖochron Laboratories, University of Göttingen, Germany for the access to the LA-SC-ICP-MS lab. The research was carried out as part of the "More efficient exploitation and use of subsurface resources" project of the University of Miskolc, implemented in the framework of the Thematic Excellence Program funded by the Ministry of Innovation and Technology of Hungary (Grant Contract reg. nr.: NKFIH-846-8/2019). We are grateful for the detailed reviews of Prof. Albrecht von Quadt, and two other reviewers Prof. Fritz Finger and Prof. Jiří Sláma whose suggestions have improved the quality of the manuscript.

Funding Open access funding provided by Eötvös Loránd University.

References

Altherr R, Albert H, Ernst H, Carola L, Hans K (1999) High-potassium, calc-alkaline I-type plutonism in the European Variscides: northern Vosges (France) and northern Schwarzwald (Germany). Lithos 50:51–73

Árva-Sós E, Balogh K (1979) Study of the granites of the Mecsek Mountains and metamorphic rocks in their surrounding by K-Ar method. Földtani Kutatás 22(4):33–36 [in Hungarian with English abstract]

Balogh K, Árva-Sós E, Gy B (1983) Chronology of granitoid and metamorphic rocks of Transdanubia (Hungary). Anuarul Institutului de Geologie şi Geofizică 61:359–364

Baxter S, Feely M (2002) Magma mixing and mingling textures in granitoids: Examples from the Galway granite, Connemara, Ireland. Mineral Petrol 76:63–74

Bea F, Montero P, Molina JF (1999) Mafic precursors, peraluminous granitoids and late lamprophyres in the Avila batholith. A model for the generation of Variscan batholiths in Iberia. J Geol 107:399–419

Bell EA, Boehnke P, Harrison TM, Wielicki MM (2018) Mineral inclusion assemblage and detrital zircon provenance. Chem Geol 477:151–160

Buda G (2001) Lamprophyre-derived vaugneritic-durbachitic mafic enclaves in Variscan granitoids from Mecsek Mts. (South Hungary). Mitt Österr Mineral Gesell 146:50

Buda G, Dobosi G (2004) Lamprophyre-derived high-K mafic enclaves in variscan granitoids from the Mecsek Mts. (South Hungary). Neu Jb Miner, Abh 180:115–147

Buda G, Nagy G (1995) Some REE-bearing accessory minerals in two types of Variscan granitoids (Hungary). Geol Carpath 46:67–78

Buda G, Pál-Molnár E (2012) Apatite as a petrogenetic indicator of Variscan granitoids in Tisza Mega-Unit (South Hungary). Carpath J Earth Env 7(4):47–60

Buda G, Lovas G, Klötzli U, Cousen BI (1999) Variscan granitoids of the Mórágy Hills (South Hungary). Eur J Mineral 11:21–32

Buda G, Puskás Z, Gál-Sólymos K, Klötzli U, Cousens BL (2000) Mineralogical, petrological and geochemical characters of crystalline rocks of the Üveghuta boreholes (Mórágy hills, South Hungary). Annual Report of Geological Institute of Hungary, pp 231–252 [in Hungarian with English abstract]

Buda G, Nagy G, Pál-Molnár E (2014) Allanite and monazite occurrences in Variscan granitoids of Tisza Mega-Unit (South Hungary). Carpath J Earth Env 9(1):57–68

Büttner S, Kruhl J (1997) The evolution of a late-Variscan high-T/low-P region: the south-eastern margin of the Bohemian Massif. Geol Rundsch 86:21–38

Chang Z, Vervoort J, McClelland W, Knaack C (2006) U-Pb dating of zircon by LA-ICP-MS. Geochem Geophys Gesyst 7(5). https://doi.org/10.1029/2005GC001100

Cherniak DJ, Watson EB (2001) Pb diffusion in Zircon. Chem Geol 172(1–2):5–24

Cherniak DJ, Watson EB (2003) Diffusion in Zircon. Rev Mineral Geochem 53:113–143

Cherniak DJ, Hanchar JM, Watson EB (1997a) Diffusion of tetravalent cations in zircon. Contrib Mineral Petrol 127:383–390

Chernüsov I (2002) Report on the K–Ar and Rb–Sr isotope age determination of the Mórágy Granite. Manuscript, Geological Institute of Hungary, Budapest [in Hungarian with English abstract]

Clemens JD (2014) Element concentrations in granitic magmas: Ghosts of textures past? J Geol Soc 171:13–19

Cocherie A, Rossi P, Fouillac AM, Vidal P (1994) Crust and mantle contributions to granite genesis an example from the Variscan batholith of Corsica, France, studied by trace-element and Nd-Sr-O-isotope systematics. Chem Geol 115:173–211

Coleman DS, Gray W, Glazner AF (2004) Rethinking the emplacement and evolution of zoned plutons: Geochronologic evidence for incremental assembly of the Tuolumne Intrusive Suite. Calif Geol 32(5):433–436

Csontos L, Vörös A (2004) Mesozoic plate tectonic reconstruction of the Carpathian region. Palaeogeogr Palaeoclimatol Palaeoecol 210:1–56

Dostal J, Murphy B, Shellnutt G, Ulrych J, Fediuk F (2019) Neoproterozoic to Cenozoic magmatism in the central part of the Bohemian Massif (Czech Republic): Isotopic tracking of the evolution of the mantle through the Variscan orogeny. Lithos 326:358–369

Dunkl I, Mikes T, Simon K, von Eynatten H (2008) Brief introduction to the Windows program Pepita: data visualization, and reduction, outlier rejection, calculation of trace element ratios and concentrations from LA-ICP–MS data. In: Sylvester P (ed) Laser ablation

ICP-MS in the Earth Sciences: current practices and outstanding issues. Short Course, Mineralogical Association of Canada 40:334–340

Ellsworth S, Navrotsky A, Ewing RC (1994) Energetics of radiation damage in natural zircon ($ZrSiO_4$). Phys Chem Miner 21:140–149

Faure M, Cocherie A, Gaché J, Esnault C, Guerrot C, Rossi P, Wei L, Qiuli L (2014) Middle Carboniferous intracontinental subduction in the Outer Zone of the Variscan Belt (Montagne Noire Axial Zone, French Massif Central): multimethod geochronological approach of polyphase metamorphism. Geological Society, London. Special Publications Geological Society of London 405:289–311

Ferre EC, Leake BE (2001) Geodynamic significance of early orogenic high-K crustal and mantle melts: example of the Corsica Batholith. Lithos 59:47–67

Foster DA, Hyndman DW (1990) Magma mixing and mingling between synplutonic mafic dikes and granite in the Idaho-Bitterroot batholiths. In: Anderson JL (ed) The Nature and Origin of Cordilleran Magmatism. Geological Society of America 174:347–358

Frei D, Gerdes A (2009) Precise and accurate in situ U-Pb dating of zircon with high sample throughput by automated LA-SF-ICP-MS. Chem Geol 261:261–270

Friedl G, Finger F, Paquette JL, von Quadt A,·McNaughton NJ, Fletcher IR (2004) Pre-Variscan geological events in the Austrian part of the Bohemian Massif deduced from U-Pb zircon ages. Int J Earth Sci 93:802–823

Gallhofer D, von Quadt A, Schmid S, Guillong M, PeytchevaI SI (2016) Magmatic and tectonic history of Jurassic ophiolites and associated granitoids from the South Apuseni Mountains (Romania). Swiss J Geosci 110:1–21

Gebauer D, Williams IS, Compston W, Grünenfelder M (1989) The development of the Central European continental crust since the Early Archean based on conventional and ionmicroprobe dating up to 3.82 b.y. old detrital zircons. Tectonophysics 157:81–96

Géczy B (1973) The origin of the Jurassic faunal provinces and the Mediterranean plate tectonics. Annales Universitatis Scientiarium Budapestinensis De Rolando Eötvös Nominatae 16:99–114

Gerdes A, Friedl G, Parrish RR, Finger F (2003) High-resolution geochronology of Variscan granite emplacement—the South Bohemian Batholith. J Czech Geol Soc 48:53–54

Götz AE, Török Á (2008) Correlation of Tethyan and Peri-Tethyan long-term and high-frequency eustatic signals (Anisian, Middle Triassic). Geol Carpath 59:307–317

Grauert B, Hänny R, Soptrajanova G (1973) Age and origin of detrital zircons from the pre-Permian basements of the Bohemian Massif and the Alps. Contrib Mineral Petrol 40:105–130

Haas J, Cs P (2004) Mesozoic evolution of the Tisza Mega-unit. Int J Earth Sci 93:297–313

Haas J, Budai T, Csontos L, Fodor L, Konrád Gy, Koroknai B (2014) Geology of the pre-Cenozoic basement of Hungary (Explanatory notes for Pre-Cenozoic geological map of Hungary, 1:500000). Geological Institute of Hungary, Budapest [in Hungarian with English abstract]

Hanchar JM, Miller CF (1993) Zircon zonation patterns as revealed by cathodoluminescence and backscattered electron images: Implications for interpretation of complex crustal histories. Chem Geol 110:1–13

Harangi S, Árváné Sós E (1993) A Mecsek hegység alsókréta vulkáni kőzetei I. Ásványtan-És Kőzettan Földtani Közlöny 123(2):129–165 [in Hungarian]

Harrison TM, Aikman A, Holden P, Walker AM, McFarlane C, Rubatto D, Watson EB (2005) Testing the Ti-in-zircon thermometer. Eos Trans AGU (program and abstracts, fall meeting 2005)

Hattori K, Sakata S, Tanaka M, Orihashi Y, Hirata T (2017) U-Pb age determination for zircons using laser ablation-ICP-mass spectrometry equipped with six multiple-ion counting detectors. J Anal At Spectrom 32:88–95

Henk A, von Blackenburg F, Finger F, Schaltegger U, Zulauf G (2000) Syn-convergent high-temperature metamorphism and magmatism in the Variscides: a discussion of potential heat sources. Geological Society, London, Special Publications 179:387–399

Holub F (1997) Ultrapotassic plutonic rocks of the durbachite series in the Bohemian Massif: petrology, geochemistry and petrogenetic interpretation. J Czech Geol Soc 31:5–26

Holub FV (1977) Petrology of inclusions as a key to petrogenesis of the durbachitic rocks from Czechoslovakia. J Czech Geol Soc 24:133–150

Hoskin PW, Schaltegger U (2003) The Composition of Zircon and Igneous and Metamorphic Petrogenesis. Rev Mineral Geochem 53:27–62

Jackson S, Pearson N, Griffin W, Belousova E (2004) The application of laser ablation-inductively coupled plasma-mass spectrometry to in situ U-Pb zircon geochronology. Chem Geol 211:47–69

Janoušek V, Rogers G, Bowes DR (1995) Sr-Nd isotopic constraints on the petrogenesis of the Central Bohemian Pluton, Czech Republic. Geol Rundsch 84:520–534

Janoušek V, Wiegand B, Žák J (2010) Dating the onset of Variscan crustal exhumation in the core of the Bohemian Massif: new U-Pb single zircon ages from the high-K calc-alkaline granodiorites of the Blatna´suite, Central Bohemian Plutonic Complex. J Geol Soc, London 167:347–360

Jantsky B (1979) Geology of granitized crystalline basement of Mecsek Mountains. Annual Report of Geological Institute of Hungary, pp 1–365 [in Hungarian with English abstract]

Jastrzębski M, Machowiak K, Krzemińska E, Lang FG, Larionov AN, Murtezi M, Majka J, Sergeev S, Ripley EM, Whitehouse M (2018) Geochronology, petrogenesis and geodynamic significance of the Visean igneous rocks in the Central Sudetes, northeastern Bohemian Massif. Lithos 316:385–405

Johnson K, Barnes CG (2006) Magma mixing and mingling in the Grayback pluton, Klamath Mountains, Oregon. In: Snoke AW, Barnes CG (eds) Geological Studies in the Klamath Mountains Province, California and Oregon: A Volume in Honor of William P. Irwin. Geological Society of America Special Paper 410:247–267

Kebede T, Kloetzli U, Koeberl C (2001) U/Pb and Pb/Pb zircon ages from granitoid rocks of Wallagga area: Constraints on magmatic and tectonic evolution of Precambrian rocks of western Ethiopia. Mineral Petrol 71:251–271

Király E, Koroknai B (2004) The magmatic and metamorphic evolution of the north-eastern part of the Mórágy Block. Annual Report of the Geological Institute of Hungary, pp 299–310 [in Hungarian with English abstract]

Kis A, Weiszburg TG, Gy B (2019) Sample prescreening methodology for increased precision U-Pb age determination of zircon. Földtani Közlöny 149(2):93–104 [in Hungarian with English abstract]

Klötzli U, Gy B, Skiöld T (2004) Zircon typology, geochronology and whole rock Sr-Nd isotope systematics of the Mecsek Mountain granitoids in the Tisia Terrane (Hungary). Mineral Petrol 81:113–134

Koroknai B, Gerdes A, Király E, Maros Gy (2010) New U-Pb and Lu-Hf isotopic constraints on the age and origin of the Mórágy Granite (Mecsek Mountains, South Hungary). IMA 20th General Meeting, 21–27 August, Budapest, Hungary, Abstracts, p 506

Kovách Á, Balogh K, Sámsoni Z (1968) Rubidium-strontium data to the problem of the age of the granites of the Mecsek Mountains. Földtani Közlöny 98(2):205–212 [in Hungarian with English abstract]

Kovács S, Szederkényi T, Haas J, Gy B, Császár G, Nagymarosi A (2000) Tectonostratigraphic terranes in the pre-Neogene basement of the Hungarian part of the Pannonian area. Acta Geol Hun 43:225–328

Kröner A, Wendt I, Liew C, Compston W, Todt W, Fiala J, Vankova V, Vanek J (1988) U-Pb zircon and Sm–Nd model ages of high-grade Moldanubian metasediments, Bohemian Massif, Czechoslovakia. Contrib Mineral Petrol 99:257–266

Kubínová Š, Faryad SW, Verner K, Schmitz M, Holub F (2017) Ultrapotassic dykes in the Moldanubian Zone and their significance for understanding of the post-collisional mantle dynamics during Variscan orogeny in the Bohemian Massif. Lithos 272:205–221

Kuşcu GG, Floyd PA (2001) Mineral compositional and textural evidence for magma mingling in the Saraykent volcanic. Lithos 50:207–230

Kusiak MA, Dunkley DJ, Suzuki K, Kachlík V, Kędzior A, Lekki J, Opluštil S (2010) Chemical (non-isotopic) and isotopic dating of Phanerozoic zircon - A case study of durbachite from the Třebíč Pluton, Bohemian Massif. Gondwana Res 17:153–161

Lee JKW, Williams IS, Ellis DJ (1997) Pb, U and Th diffusion in natural zircon. Nature 390(6656):159–162

Lelkes-Felvári G, Frank W (2006) Geochronology of the metamorphic basement, Transdanubian part of the Tisza Mega-Unit. Acta Geol Hun 49(3):189–206

Lowenstern J, Persing H, Wooden J, Lanphere M, Donnelly-Nolan J, Grove T (2000) U-Th dating of single zircons from young granitoid xenoliths: new tools for understanding volcanic processes. Earth Planet Sci Lett 183:291–302

Ludwig KR (2012) Isoplot. Berkeley Geochronology Center, Special Publication, A geochronological toolkit for Microsoft Excel, p 5

Marsellos A, Garver J (2010) Radiation damage and uranium concentration in zircon as assessed by Raman spectroscopy and neutron irradiation. Am Miner 95:1192–1201

Maros Gy, Koroknai B, Palotás K, Fodor L, Dudko A, Forián-Szabó M, Zilahi-Sebess L, Bán-Győry E (2004) Tectonics and structural history of the north-eastern Mórágy Block. Annual Report of Geological Institute of Hungary, pp 371–394 [in Hungarian with English abstract]

Mezger K, Krogstad EJ (1997) Interpretation of discordant U-Pb zircon ages: An evaluation. J Metamorph Geol 15:127–140

Murakami T, Chakoumakos BC, Ewing RC (1986) X-ray powder diffraction analysis of alpha-event radiation damage in zircon ($ZrSiO_4$). In: Clark DE, White WB, Machiels AJ (eds) Nuclear waste management II. Advances in Ceramics 20:745–753. American Ceramic Society, Columbus, Ohio

Nasdala L, Irmer G, Wolf D (1995) The degree of metamictization in zircons: a Raman spectroscopic study. Eur J Mineral 7:471–478

Nasdala L, Pidgeon RT, Wolf D, Irmer G (1998) Metamictization and U-Pb isotopic discordance in single zircons: a combined Raman microprobe and SHRIMP ion probe study. Mineral Petrol 62:1–27

Nasdala L, Wenzel M, Vavra G, Irmer G, Wenzel T, Kober B (2001) Metamictisation of natural zircon: accumulation versus thermal annealing of radioactivity-induced damage. Contrib Mineral Petrol 141:125–144

Nemchim AA, Cawood PA (2005) Discordance of the U-Pb system in detrital zircons: Implication for provenance studies of sedimentary rocks. J Sediment Geol 182:143–162

Neves SP, Vauchez A (1995) Successive mixing and mingling of magmas in a plutonic complex of northeast Brazil. Lithos 34:275–299

Nutman AP, Maciejowski R, Wan Y (2014) Protoliths of enigmatic Archaean gneisses established from zircon inclusion studies: case study of the Caozhuang quartzite, E. Hebei. China Geosci Front 5:445–455

Ovchinnikov LN, Panova MB, Shangareev FL (1965) Absolutnyi vozrast nekotoryh geologicheskikh obrazovanii Vengrii [in Russian with English abstract: Absolute age of some geological formations of Hungary]. Acta Geologica Academiae Scientiarum Hungarici 9(3–4):305–312

Paces JB, Miller JD (1993) Precise U-Pb ages of Duluth Complex and related mafic intrusions, northeastern Minnesota: geochronological insights into physical, petrogenetic, paleomagnetic and tectonomagmatic processes associated with the 1.1 Ga midcontinent rift system. J Geophys Res 98:13997–14013

Parat F, Holtz F, René M, Almeev R (2009) Experimental constraints on ultrapotassic magmatism from the Bohemian Massif (durbachite series, Czech Republic). Contrib Mineral Petrol 159:331–347

Peytcheva I, Quadt A, Georgiev N, Ivanov Zh, Heinrich CA, Frank M (2008) Combining trace-element compositions, U-Pb geochronology and Hf isotopes in zircons to unravel complex calcalkaline magma chambers in the Upper Cretaceous Srednogorie zone (Bulgaria). Lithos 104:405–427

Pearson ES (1939) "Student" as statistician. Biometrika 30(3/4):210

Pidgeon R, Nemchin A, Hitchen G (1998) Internal structures of zircons from Archaean granites from the Darling Range batholith: implications for zircon stability and the interpretation of zircon U-Pb ages. Contrib Mineral Petrol 132:288–299

Pupin JP (1980) Zircon and granite petrology. Contrib Mineral Petrol 73:207–220

Putnis A (2009) Mineral replacement reactions. In: Putirka KD, Tepley FJ (eds) Minerals, inclusions and volcanic processes. Rev Mineral Geochem, vol 70. Mineralogical Society of America, Chantilly, pp 87–124

Sabatier H (1991) Vaugnerites: Special lamprophyre-derived mafic enclaves in some Hercynian granites from Western and Central Europe. In: Didier J, Barbarin B (eds) Enclaves and granite petrology. Elsevier, Amsterdam, pp 63–81

Sambridge MS, Compston W (1994) Mixture modeling of multicomponent data sets with application to ion-probe zircon ages. Earth Planet Sci Lett 128(3–4):373–390

Sauer A (1892) The granitite of Durbach in the northern Black Forest and its border facies of Glimmersyenit (durbachite). Mitteilungen Der Grossherzoglich Badischen Geologischen Landesanstalt 2:231–276 [in German with English abstract]

Schiller D, Finger F (2019) Application of Ti-in-zircon thermometry to granite studies: problems and possible solutions. Contrib Mineral Petrol 174:51

Schmid SM, Bernoulli D, Fügenschuh B, Matenco L, Schefer S, Schuster R, Tischler M, Ustaszewski K (2008) The Alpine–Carpathian–Dinaridic orogenic system: correlation and evolution of tectonic units. Swiss J Geosci 101:139–183

Schmitt AK, Stockli DF, Lindsay JM, R. Robertson R, Lovera M, Kislitsyn R (2010) Episodic growth and homogenization of plutonic roots in arc volcanoes from combined U-Th and (U-Th)/He zircon dating. Earth Planet Sci Lett 295:91–103

Shatagin K, Chernyshev I, Balla Z (2005) Geochronology of Mórágy Granite: Results of U-Pb, Rb-Sr, K-Ar and 40Ar-39Ar isotope study. Annual Report of Geological Institute of Hungary, pp 41–64 [in Hungarian with English abstract]

Sláma J, Košler J, Condon DJ, Crowley JL, Gerdes A, Hanchar JM, Horstwood MSA, Morris GA, Nasdala L, Norberg N, Schaltegger U, Schoene B, Tubrett MN, Whitehouse MJ (2008) Plešovice zircon—a new natural reference material for U-Pb and Hf isotopic microanalysis. Chem Geol 249:1–35

Svingor É, Kovách Á (1981) Rb–Sr isotopic studies on granodioritic rocks from the Mecsek Mountains. Hungary Acta Geologica Academiae Scientiarum Hungarici 24(2–4):295–307

Szederkényi T (1977) Geological evolution of South Transdanubia (Hungary) in Paleozoic time. Acta Mineral Petrol Szeged 23(1):3–14

Szederkényi T (1996) Metamorphic Formations and Their Correlation int he Hungarian Part of Tisia Megaunit (Tisia Composite Terrane). Acta Mineral Petrol, pp 143–160

Szederkényi T, Haas J, Nagymarosy A, Hámor G (2012) Geology and History of Evolution of the Tisza Mega-Unit. Geology of Hungary. Springer Berlin Heidelberg, pp 48–103. https://doi.org/10.1007/978-3-642-21910-8_2

Szymanowski M, Jancewicz K, Migoń P, Różycka M (2018) How large-scale geomorphometric approach can contribute to detect erosional signals in complex geomorphic landscapes – The role of expert decisions in multivariate unsupervised relief classification. https://doi.org/10.13140/RG.2.2.26095.28329

Szulc J (2000) Middle Triassic evolution of the northern Peri-Tethys area as influenced by early opening of the Tethys ocean. ASGP 70:1–48

Tari G (2015) The palinspastic position of Tisia (Tisza) in the Alpine realm: a view from the outside of the Pannonian Basin. In: Dálya V, Sámson M (eds) Tisia Conference, Pécs, 27–28. February 2015. Molnár Printing and Publishing, Pécs, pp 29–32 [in Hungarian with English abstract]

Van Breemen O, Aftalion M, Bowes D, Dudek D, Misai Z, Povondra P, Vrána S (1982) Geochronological studies of the Bohemian massif, Czechoslovakia, and their significance in the evolution of Central Europe. Transactions of the Royal Society of Edinburgh. Earth Sci 73:89–108

Van Lankvelt A, Schneider DA, Biczok J, McFarlane CRM, Hattori K (2016) Decoding Zircon Geochronology of Igneous and Alteration Events Based on Chemical and Microstructural Features: a Study from the Western Superior Province, Canada. J Petrol 57:1309–1334

Ventura G, Del Gaudio P, Iezzi G (2006) Enclaves provide new insights on the dynamics of magma mingling: A case study from Salina Island (Southern Tyrrhenian Sea, Italy). Earth Planet Sci Lett 243:128–140

von Quadt A, Gallhofer D, Guillong M, Peytcheva I, Waelle M, Sakata S (2014) U-Pb dating of CA/non-CA treated zircons obtained by LA-ICP-MS and CA-TIMS techniques: impact for their geological interpretation. J Anal At Spectrom 29:1618–1629

von Quadt A, Erni M, Martinek K, Moll M, Peytcheva I, Heinrich CA (2011) Zircon crystallization and the lifetimes of ore-forming magmatic-hydrothermal systems. Geology 39:731–734

Von Raumer JF, Janousek V, Stampfli GM (2012) Durbachites Vaugnerites – a time-marker across the European Variscan basement. Geol France 1:178–180

Von Raumer JF, Finger F, Veselá P, Stampfli GM (2014) Durbachites-Vaugnerites - a geodynamic marker in the central European Variscan orogen. Terra Nova 26:85–95

Watson EB, Wark DA, Thomas JB (2006) Crystallization thermometers for zircon and rutile. Contrib Mineral Petrol 151:413–433

Weinschenk E (1916) The fundamental principles of petrology. Translation by Albert Johannsen, New York Mc Graw-Hill Book Company

Wendt JI, Kröner A, Fiala J, Todt W (1993) Evidence from zircon dating for existence of approximately 2.1 Ga old crystalline basement in southern Bohemia. Czech Republic Geol Rundsch 82:42–50

Wetherill GW (1956) Discordant uranium-lead ages. Trans Amer Geophys Union 37:320–326

Woensdregt CF (1992) Computation of surface energies in an electrostatic point charge model. II. Application to zircon ($ZrSiO_4$). Phys Chem Miner (19/1):59–69

Woodhead JA, Rossman GR, Silver LT (1991) The metamictization of zircon: Radiation dose-dependent structural characteristics. Am Mineral 76:74–82

Wotzlaw JF, Schaltegger U, Frick DA, Dungan MA, Gerdes A, Gunther D (2013) Tracking the evolution of large-volume silicic magma reservoirs from assembly to supereruption. Geology 41:867–870

Žák J, Verner K, Janoušek V, Holub FV, Kachlík V, Finger F, Hajná J, Tomek F, Vondrovic L, Trubac J (2014) A plate-kinematic model for the assembly of the Bohemian Massif constrained by structural relationships around granitoid plutons. In: Schulmann K, Martínez Catalán JR, Lardeaux JM, Janoušek V, Oggiano G (eds) Special Publications, Geological Society, London, United Kingdom

Zhang M, Salje EKH (2001) Infrared spectroscopic analysis of zircon: Radiation damage and the metamict state. J Phys: Condensed Matter 13:3057–3071

Zhang M, Salje EKH, Farnan I, Graeme-Barber A, Daniel P, Ewing RC, Clark AM, Lennox H (2000) Metamictization of zircon: Raman spectroscopic study. J Phys: Condensed Matter 12:1915–1925

Zoubek V (1988) Precambrian in younger fold belts, European Variscides, the Carpathians and Balkans. Wiley, New York, pp 1–37

Zwart HJ (1986) The Prevariscan basement in the European Variscan Belt. In: Freeman R, Mueller ST, Giese P (eds) European Geotraverse Workshop. European Science Foundation, Strasbourg, France, pp 25–31